Crustal structure of the Innuitian region of Arctic Canada and Greenland from gravity modelling: implications for the Palaeogene Eurekan orogen

Gordon N. Oakey[1] and Randell Stephenson[2]

[1]*Geological Survey of Canada, Halifax, Canada. E-mail: GOakey@nrcan.gc.ca*
[2]*VU University Amsterdam, the Netherlands*

SUMMARY

New gravity observations collected over Ellesmere Island and Axel Heiberg Island have been integrated with existing Canadian and Danish data sets to produce a comprehensive regional compilation over the Innuitian Region of the Canadian and Greenland High Arctic. This compilation has provided quantitative assessment of the geometry of the plate boundary between northern Greenland and Ellesmere Island and crustal structures across the Cretaceous–Palaeogene Eurekan Orogen.

A large amplitude linear gravity low—Nares Strait Gravity Low (NSGL) (<-160 mGal)—extends obliquely across Nares Strait from northern Greenland to Ellesmere Island. This feature closely correlates with the distribution of the Palaeozoic Franklinian Margin sequences and is cross-cut by the Cenozoic Eurekan Frontal Thrust (EFT), which represents the mappable western limit of the undeformed Greenland Plate associated with the Eurekan Orogen. Newly identified linear gravity features occur north of the NSGL: the Hazen Plateau Gravity High (HPGH), corresponding with the low-lying topography of the Hazen Trough and the Grantland Gravity Low (GGL), over the elevated topography of the Grantland Uplift.

Gravity models for profiles crossing the NSGL, the HPGH and the GGL indicate that the long-wavelength component of the gravity anomalies is produced by systematic variations in Moho depth. Although significant Eurekan-age thrusting and thickening of low-density Palaeozoic strata is observed on Ellesmere Island, locally contributing to the mass-deficit generating the NSGL, equivalent strata on Greenland are undeformed. The NSGL is interpreted to be primarily the signature of the remnant (Early Palaeozoic) margin with the downwards flexure of the crust beneath a northwards thickening sedimentary wedge rather than purely the result of crustal thickening from the Eurekan Orogeny.

Digital bathymetry and sediment thickness data were used to determine a residual 'crustal' gravity field, which in turn was used to calculate depth-to-Moho and crustal thicknesses. These have been interpreted in terms of crustal affinity and crustal thinning and thickening processes associated with the Late Cretaceous–Palaeogene plate tectonics of the area. Significant crustal thinning is observed beneath the Lancaster Basin, between Baffin Island and Devon Island, corresponding with 40 km of separation. This is interpreted to be a failed rift-arm of the Eocene spreading system in Baffin Bay.

A Fourier-domain transfer function analysis (Q) determined an intermediate average crustal strength (flexural rigidity of 10^{22} N m) over the Innuitian region. Comparisons with theoretical models, based on a simple thin elastic plate model, suggest that the crust is relatively thin (30 km) and in near-isostatic equilibrium—that is, not flexurally supporting the existing sedimentary or topographic load. A clearly defined anisotropy is identified, correlating with the direction of Eocene plate convergence, suggesting that the Eurekan collisional forces have not yet dissipated and are at least partially supporting large-scale orogenic structures.

Key words: Gravity anomalies and Earth structure; Continental tectonics: compressional; Continental tectonics: strike-slip and transform; Dynamics: gravity and tectonics; Lithospheric flexure; Arctic region.

1 INTRODUCTION

During the development of the North Atlantic, the Late Cretaceous–Palaeogene motion of Greenland relative to North American produced complex intraplate tectonic episodes in the Nares Strait region of the Canadian-Greenland High Arctic (Fig. 1). Although a discrete linear plate boundary—the Wegener Fault—within the Nares Strait waterway (Wegener 1915) has been used in plate kinematic reconstructions to accommodate up to 300 km of sinistral strike-slip motion (Srivastava & Tapscott 1986), convergence between Greenland and Ellesmere caused complex reactivation of Palaeozoic and Proterozoic structures with significant compressional deformation and orogenic uplift within the Canadian Arctic Islands—the Eurekan Orogeny. A large gravity low over central Nares Strait—the Nares Strait Gravity Low (NSGL)—was identified by Jackson & Koppen (1985) and interpreted by these authors to be the result of crustal thickening associated with a subduction zone along a convergent intercontinental margin. The details of timing and geometry of the orogen have been enigmatic due to reactivation of older structures, large gaps in geophysical mapping, limited onshore–offshore geological mapping and poorly constrained plate tectonic models.

In this paper, a new gravity compilation over the Innuitian Region of northern Canada and Greenland from the Canada–Greenland Map Series (Oakey *et al.* 2001a) is presented and used to define regional-scale geological structures and provide better constraints on the geometry of the overprinted Eurekan Orogeny. The new gravity data have provided continuous mapping of the NSGL across Nares Strait, allowing for an improved assessment of its relationship with the plate boundary between Greenland and Ellesmere Island. Further, the gravity data have been integrated with newly compiled bathymetric data (Oakey *et al.* 2001b) as well as with a regional sediment thickness grid that was compiled from a mosaic of academic and industry sources. This has facilitated mapping the onshore–offshore continuity of geological structures and has allowed a series of quantitative analyses—including depth-to-Moho and crustal thinning estimations, forward modelling and isostatic admittance—to be undertaken to support a regional interpretation of the study area in terms of crustal affinity and tectonic evolution.

2 GEOLOGY AND TECTONIC HISTORY OF THE INNUITIAN REGION

The geology of the Innuitian Region (Fig. 2), crossing Nares Strait between Greenland and Canada, records multiple orogenic events dating back to the Archaean, often making it difficult to differentiate the complex overprinting of structural elements. The youngest major tectonic event is the Palaeogene Eurekan Orogeny, which is the main focus of this paper.

2.1 Regional geology

The onshore geology of coastal areas of northern Baffin Bay is dominated by Archaean and Paleoproterozoic crystalline rocks comprising numerous complex terranes. Overlying Mesoproterozoic sedimentary sequences including the Thule Supergroup and equivalents of the Borden Basin are broadly distributed on Greenland, Ellesmere Island and Baffin Island and have been mapped offshore in southernmost Nares Strait and Kane Basin (KB). A passive continental margin (the Franklinian Margin) lay along the Precambrian craton by latest Proterozoic–Early Palaeozoic times and subsequently 'closed'

during Devonian orogenesis. Trettin (1989) divided the Palaeozoic record of the Innuitian Region into regional successions. These are Late Neoproterozoic–Cambrian and younger carbonate rocks of the Arctic Platform and the Cambrian–Devonian aged successions of the shelf and deep-water 'provinces', the former dominated by carbonate sequences and the latter subdivided into sedimentary and volcano-sedimentary sequences. These units were affected by multiple tectonic events culminating in the Late Devonian–Early Carboniferous Ellesmerian Orogeny. The exotic, stratigraphically and structurally complex, Pearya Composite Terrane constitutes most of northern Ellesmere Island and is thought to represent an assemblage of continental fragments accreted to the North American Plate during the Palaeozoic (Trettin 1991).

The Sverdrup Basin is a post-Ellesmerian Orogeny intracratonic (or 'successor') basin (Stephenson *et al.* 1987) approximately 1300 km long and up to 400 km wide with over 2 km of Upper Palaeozoic strata (Davies & Nassichuk 1991) and up to 8 km of Mesozoic strata (Embry 1991). Much of the Mesozoic section is intruded by Cretaceous mafic sills and dykes, as well as salt diapirs. Magmatism has been associated with the opening of Canada Basin and the development of the present polar continental margin of Canada (Embry 1991). The Sverdrup Basin culminates with the non-marine Eureka Sound Group (Ricketts 1986; Miall 1991), locally controlled by Late Cretaceous–Palaeogene fault systems of the Eurekan Orogeny (Okulitch *et al.* 1990). These fault systems often represent reactivated Ellesmerian and older structures (Phillips 1990). The uppermost Neogene to Recent succession, the Arctic Coastal Plain, is a wedge of seaward deepening fluvial and marine sequences deposited along the modern northern passive continental margin.

2.2 Mesozoic and Cenozoic basins

Cretaceous rifting (pre-seafloor spreading) between Greenland and Canada developed syn-rift marginal basins extending from the Labrador Sea (Balkwill 1990; Chalmers & Puvertaft 2001) to the Innuitian Region (Okulitch & Trettin 1991). The locations of the major basins surrounding northern Baffin Bay are shown in Fig. 2. Half-graben basins on both the Baffin shelf (Jackson *et al.* 1992) and Melville Bay (Whittaker & Hamann 1995) on the Greenland margin, are also thought to contain Cretaceous syn-rift sediments. The deep inner Melville Bay Graben (MBG) is separated from the North and South Kivioq basins (NKB and SKB) by the Melville Bay Ridge. Both basins are deeper in the south, and structurally divided from the northern ends of the basins. Narrow elongated basins northwest of the MBG extend to the Carey Basin (CB) and show evidence of inversion. The CB is a north–south oriented basin with strata that has had significant basin inversion and overprinting of 'flower-structures' (Jackson *et al.* 1992). To north of CB is the NW–SE oriented North Water Basin (NWB). The Glacier Basin (GB) is a narrow N–S oriented basin with only a thin layer of low velocity strata. Within KB, the shallow Franklin Pierce Basin (FPB) is structurally bounded to the west by the Eurekan Frontal Thrust.

Upper Cretaceous successions are locally exposed onshore in the north Baffin region (e.g. Miall 1991). The EW oriented Devon Arch (DA) forms a structural divide between stepped faults dipping north towards Jones Sound and south towards Lancaster Sound (Okulitch & Trettin 1991) at the northwestern margin of Baffin Bay and can therefore be considered as a 'mega-horst'. The geometry of the Jones Sound Basin (JSB) is poorly known whereas the Lancaster Basin
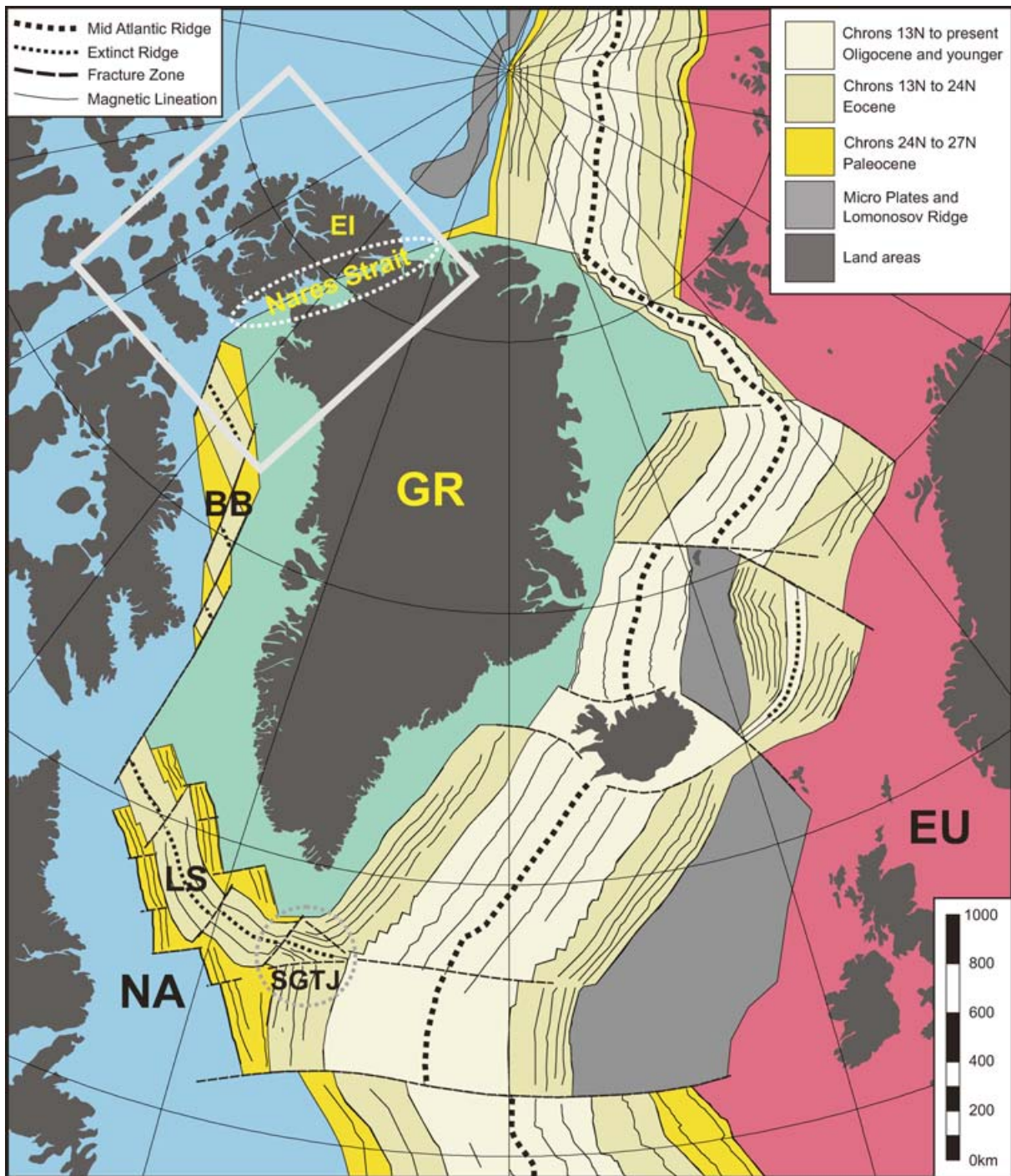
Figure 1. The North Atlantic spreading system. The Innuitian Region (grey box) includes Northern Greenland, and crosses Nares Strait to the Canadian land area of Ellesmere Island (EI). Intraplate tectonics resulting from relative motions between the Greenland Plate (GR; green) and the North American Plate (NA; blue) can be constrained by the age and geometry of the now-extinct seafloor spreading system within Labrador Sea (LS) and Baffin Bay (BB). During the Eocene, GR moved as an independent plate between NA and Eurasia (EU; red). The motion between GR and NA terminated at the end of the Eocene (chron 13N) based on the identification of magnetic anomalies associated with the South Greenland Triple Junction (SGTJ).

(LB) is mapped as a half graben dipping northwards and bounded against a steeply dipping normal fault (the Parry Channel Fault, Kerr 1980). The Lancaster Basin, Bylot Basin (BB) and Lady Anne Basin (LAB) are separated by NW–SE oriented basement ridges (Rice & Shade 1982) (see also Fig. 8 for locations).

2.3 Eurekan orogeny

Active tectonism, related to the opening of the northern Atlantic Ocean, first between Greenland and Canada and thereafter east of Greenland (e.g. Fig. 1) affected the Innuitian Region in latest
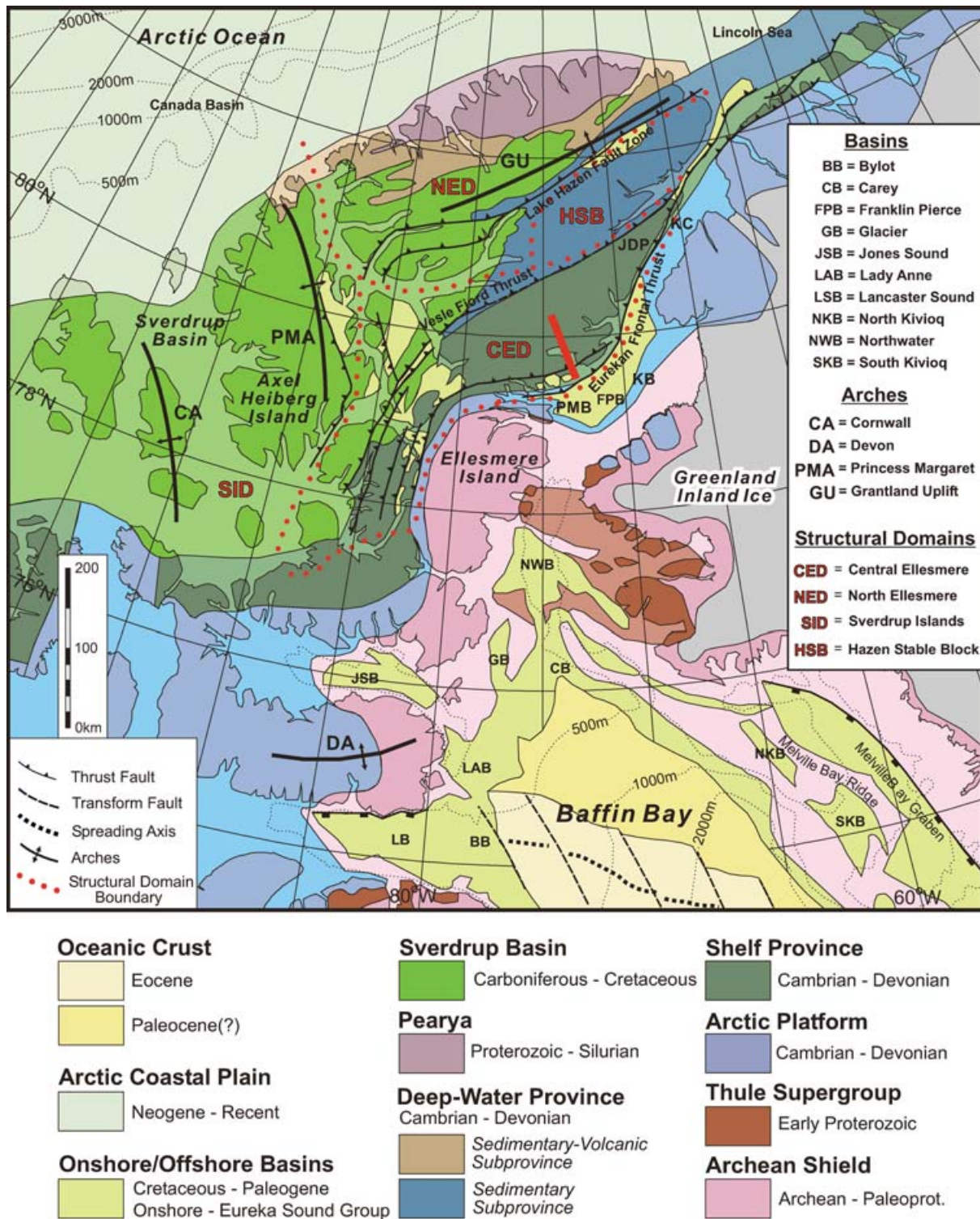
Figure 2. Geological map of the Innuitian region. Onshore geology is based mainly on Trettin (1991). The geometry of the Baffin Bay rift system and Eocene crust is from Oakey (2005) and the position of the Eurekan Frontal Thrust (EFT) is adapted from Harrison *et al.* (2006). Sedimentary basins and tectonic elements mentioned in the text are labelled as shown along with the main structural domains of the Eurkean Orogen. The red line indicates the location of the geological cross-section seen in Fig. 3. JDP, Judge Daly Promontory; KB, Kane Basin; KC, Kennedy Channel; PCM, Princess Marie Bay.

Cretaceous–Palaeogene times. Deformations associated with this tectonism are sometimes collectively referred to as 'Eurekan', although, strictly speaking, the term 'Eurekan Orogen' should be limited to compressional (shortening) structures developed exclusively

during the Eocene (Tessensohn & Piepjohn 1998). The edge of the Eurekan (Eocene) deformation is defined along the Eurekan Frontal Thrust (EFT; Okulitch & Trettin 1991; Harrison 2006), which represents the easternmost thrust fault of a complex imbricate thrust
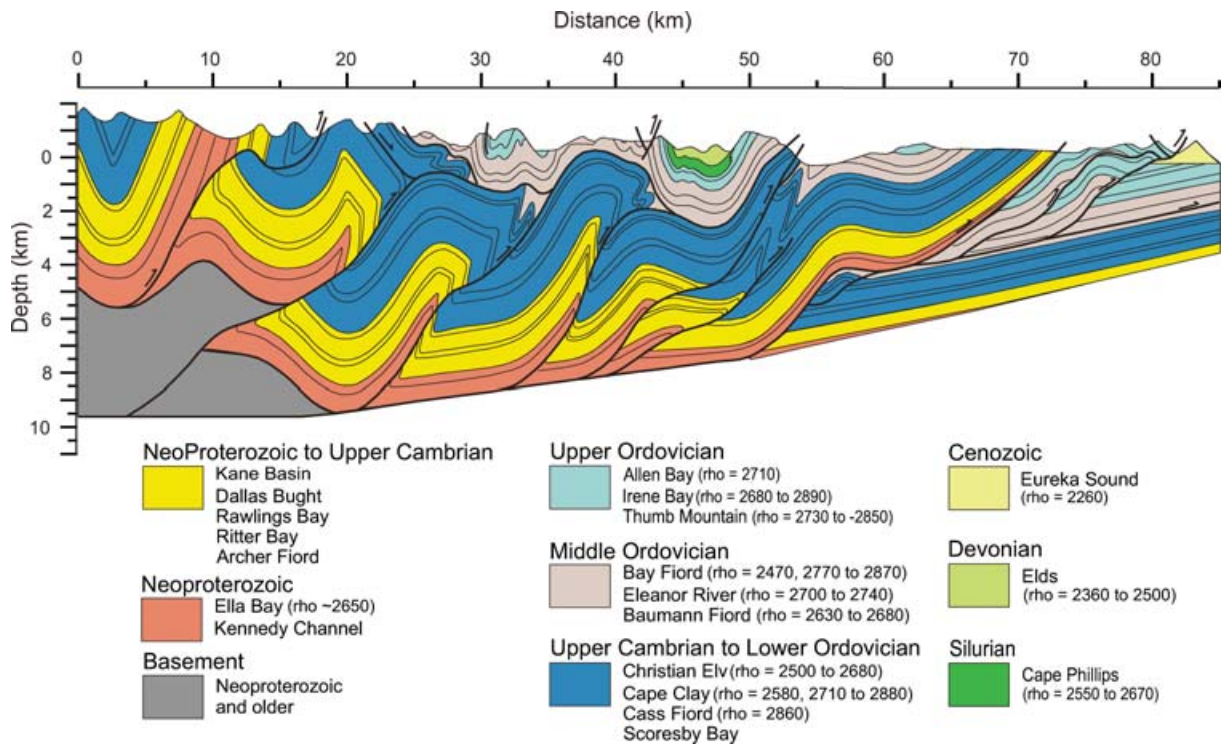
Figure 3. Balanced geological cross-section across the Central Ellesmere Domain showing Eurekan folds and thrusts (Harrison & de Freitas, 2007), located in Fig. 2. Vertical exaggeration is 2:1. Densities ('rho') tabulated in the legend have units of kg m^{-3} and were used in the gravity modelling (Section 5.2). Approximately 100 km of shortening is estimated across the section.

fault zone. The associated deformation is restricted to the Canadian side of the EFT, and equivalent strata onshore Greenland are generally undeformed (Peel & Christie 1982). A balanced geological cross-section in the vicinity of KB (Harrison & de Freitas 2007) is shown in Fig. 3. Most of the approximately 100 km of shortening estimated across the section is attributed to Eurekan deformation. The EFT is mapped near-shore Ellesmere Island in Kennedy Channel (KC) from shallow seismic and bathymetric profiles (Jackson *et al.* 2006). A fault-bounded basin along the eastern shore of Judge Daly Promontory (JDP) (Saalman *et al.* 2005) contains sandstones and conglomerates with a high proportion of basalt clasts (Saalman *et al*. in press). The associated magnetic anomaly can be traced from on-shore JDP northeast into the Lincoln Sea (Damaske & Oakey 2006). Basement structures from Greenland to Ellesmere Island mapped by aeromagnetics across KB (Oakey & Damaske 2006) indicate that the Archaean crustal 'block' of southeast Ellesmere Island is part of the Greenland Plate and that the EFT does not continue as a simple linear feature to the south as suggested by Hood *et al.* (1985). Harrison *et al.* (2006) map the EFT along the northern coast of Princess Marie Bay (PMB) westwards to link with the thrust faults mapped along the western edge of the Archaean crustal block of southeastern Ellesmere Island.

Okulitch & Trettin (1991) described the Eurekan Orogeny in terms of four structural domains, as seen in Fig. 2. The Sverdrup Island Domain (SID) has predominantly E- and NE-vergent thrusts with associated folds, faults and salt diapirism. Two N–S oriented structural highs, the Cornwall Arch (CA) and the Princess Margaret Arch (PMA), which are associated with localized uplift within the Sverdrup Basin, were interpreted by Forsyth *et al.* (1979), from regional refraction seismic data, and Stephenson & Ricketts (1990), from gravity data, to be caused by crustal scale folding. Ricketts

& Stephenson (1994) attributed an Eocene age to the arch uplift. The Northern Ellesmere Domain (NED) is dominated by en echelon SE-vergent thrust systems bounded by the Lake Hazen Fault Zone. Limited dextral motion is inferred on some of these faults. Structures in the NED range from Palaeozoic to Palaeogene in age, with numerous examples of reactivated structures (Trettin 1991). Within the NED is the EW oriented Grantland Uplift, a broad topographic high with a complex geology associated with the suture zone of the Pearya Composite Terrane and including remnants of the Sverdrup Basin strata. The Hazen Stable Block (HSB) has horizontal Palaeogene Eureka Sound Group strata overlying steeply dipping beds of the Palaeozoic Hazen Fold Belt (Christie 1976), implying only minor Eurekan-aged deformation. It is geographically coincident with the low-lying Hazen Trough. The Central Ellesmere Domain (CED) represents the deformation zone directly associated with the EFT. It is characterized by extensive E- and SE-vergent thrust faults with associated folds forming a typical foreland fold-and-thrust belt of Eurekan age but incorporating strata predating the Devonian-Carboniferous Ellesmerian Orogeny (i.e. sediments of the Palaeozoic 'shelf province' defined above).

2.4 Late Cretaceous–Palaeogene plate kinematics and tectonic framework

The post-Palaeozoic tectonic development of the Innuitian Region can be summarized by four distinct episodes that are directly linked to the development of the Late Mesozoic intercontinental and Cenozoic oceanic rift system between Greenland and Canada (Fig. 4). These are: (1) pre-Eurekan rifting, basin development and volcanic intrusions during the Late Cretaceous; (2) intense sinistral faulting and regional uplift during the Paleocene; (3) Eurekan folding
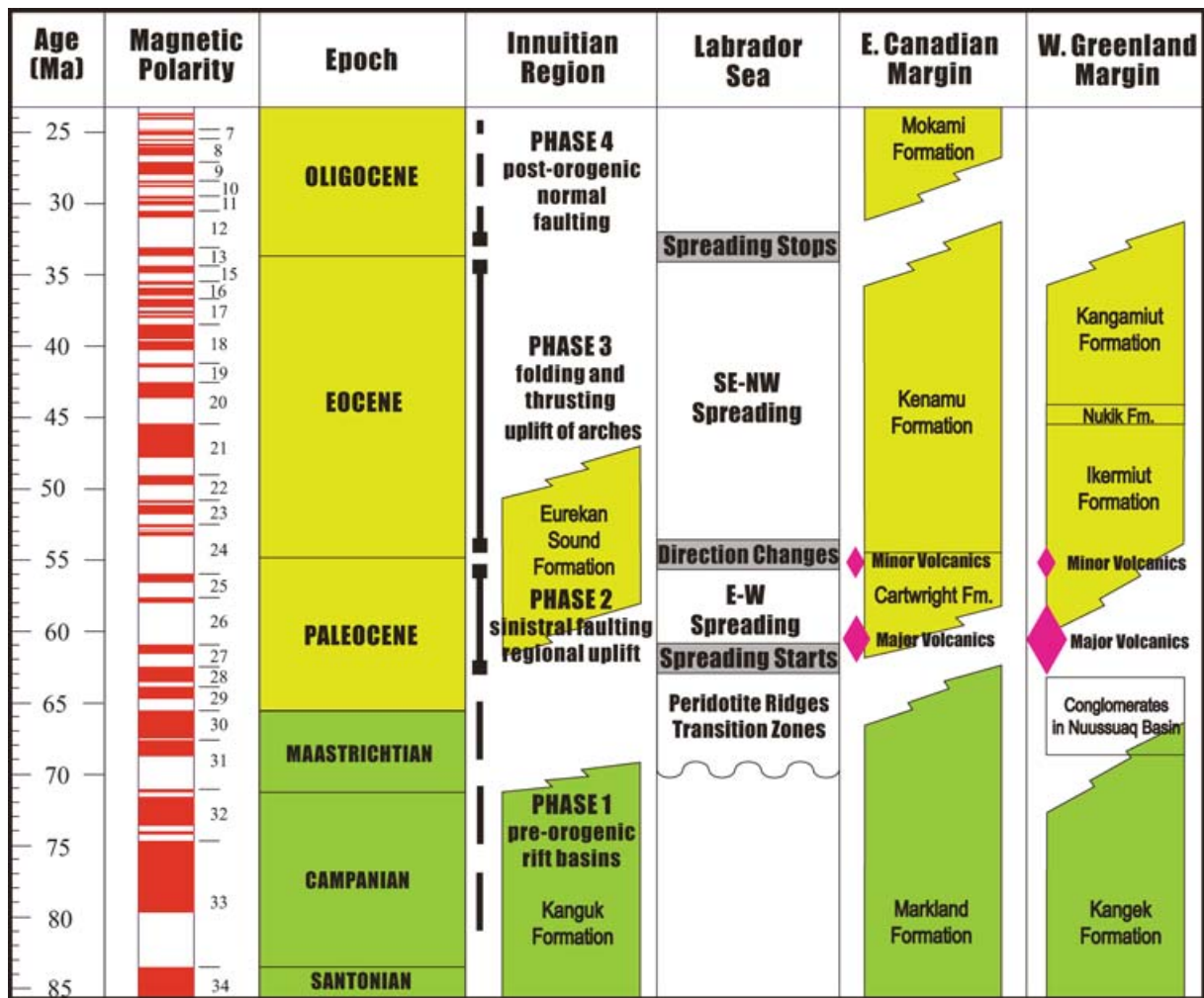
Figure 4. Tectonic phases of the Innuitian Region (adapted from Miall, 1991) compared with tectonic episodes recognized in the Labrador Sea–Baffin Bay rift history and stratigraphic elements of the SE Greenland and Labrador margins (adapted from Chalmers & Pulvertaft 2001). The magnetic and geological timescales are from Hardenbol *et al.* (1998)

and thrusting during the Eocene and 4) post-orogenic collapse with localized normal faulting and salt diapirism. These four tectonic phases are consistent with plate kinematic models constrained by the geometry of 'seafloor spreading' magnetic anomalies in the Labrador Sea (e.g. Srivastava 1978; Roest & Srivastava 1989). More recently, Oakey (2005) and Oakey & Chalmers (submitted) have provided improved estimates of the orientation and magnitudes of plate motions in the Innuitian Region by incorporating the geometry of fracture zones in Baffin Bay (e.g. Fig. 1).

During Phase 2 (Paleocene), approximately 170 km of separation occurred between Greenland and Baffin Island, producing oceanic crust within Baffin Bay accompanied by Paleocene sinistral faulting (Tessensohn & Piepjohn 1998) in the Nares Strait area and broad regional uplift, attributed to mantle plume activity (Harrison *et al.* 1999). A dramatic change in spreading direction occurred during the magnetic chron 24R (Paleocene–Eocene boundary), corresponding with the timing of the initiation of oceanic spreading along the east Greenland margin. Within Baffin Bay, highly oblique seafloor spreading continued during the Eocene (Phase 3) and convergence occurred between northern Greenland and Ellesmere Island. The new kinematic model (Oakey 2005; Oakey & Chalmers, submitted) defines approximately 250 km of

Eocene convergence, which is substantially more than the observed shortening in the structural cross-section (Fig. 3). This discrepancy suggests that additional processes must be considered, possibly explained by a combination of crustal folding and reactivation of Ellesmerian structures across the Sverdrup Basin and/or the Grantland Uplift, as well as localized extension associated with the oceanic rift system. In Central Ellesmere Island, the predominant structural fabric found from the statistical analysis of fault systems (Oakey 1994) is consistent with a single episode of convergence. The direction defined by Roest & Srivastava's (1989) kinematic model suggests pure compression; however, the new model (Oakey 2005; Oakey & Chalmers, submitted) suggests a minor (sinistral) strike-slip component.

The ridge structures separating the subbasins in the Lancaster Sound area (LB, BB and LAB) are oriented parallel to the direction of Eocene motion of the Greenland Plate. Their orientations are also consistent with the direction of Paleocene rifting. As such, it is uncertain whether basin geometry is dominated by the Paleocene extension, Eocene inversion or a combination of both. The strata within all three subbasins exhibit a pronounced angular unconformity at the seafloor, but only the LAB has been overprinted by compressive deformation (Jackson *et al.* 1992).

The end of the Eurekan Orogeny is constrained by the Late Eocene (magnetic chron13N) extinction of the seafloor spreading in Labrador Sea and the termination of the South Greenland Triple Junction (see Fig. 1). Post-orogenic collapse (Phase 4; Fig. 4) is documented by regionally extensive normal faulting (DePaor 1989; Trettin 1991).

3 DATA

3.1 Physiography (topography and bathymetry)

The topographic and bathymetric (physiography) data used in this study (Fig. 5) are from Oakey *et al.* (2001b), compiled from a variety of Canadian and Danish sources. Topographic data for most of the Canadian land area was provided by the United States Geologi-cal Survey (GTOPO30 1999). Topographic data over Ellesmere and Axel Heiberg islands were from 1:250000 scale digital contours maps (Geogratis 2008). Gridded topographic data for Greenland were provided by the Danish National Survey and Cadastre (1998). Bathymetric data were assembled from combined marine survey tracks (Earth Physics Branch 1985), point values from gravity stations (Canadian Geophysical Data Centre 2000; Danish National Survey and Cadastre 1998) and digital archives from the Canadian Hydrographic Service (CHS) (Whire, K. Personal Communications 1998). GEBCO digital bathymetric contours (Jones *et al.* 1994) were used in the Arctic Ocean and Melville Bay, where digital point data were sparse. Data sources are shown in Fig. 6a.

The physiography of the Innuitian Region, generally reflects differences in bedrock geology and structures, which influence different styles of erosion, as outlined by Dawes & Christie (1991).
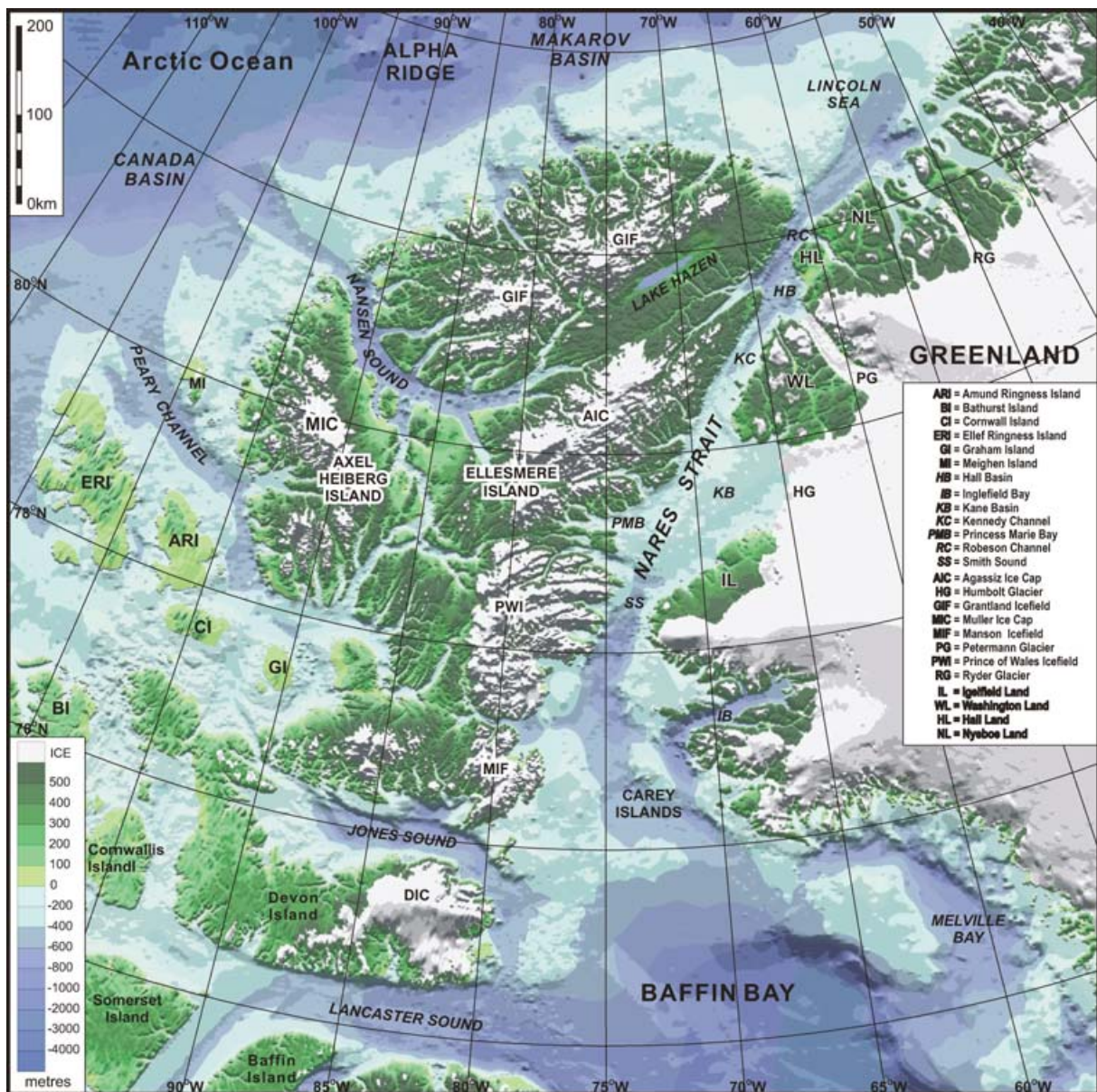

Figure 5. Physiography of the Innuitian Region; digital topography and bathymetry data have been combined from a number of sources (see Fig. 6a) to produce a regional digital terrain model (DTM) to visualize the physiography of the Innuitian Region of the Canadian and Greenland High Arctic (Oakey *et al.* 2001b). This false-coloured image is illuminated from the north with colour changes representing contours of elevation or bathymetric depth. The distribution of ice, shown in white, has been defined with a gridded mask for Greenland (Ekholm 1996) and polygons for Canada (Digital Chart of the World, 1992).
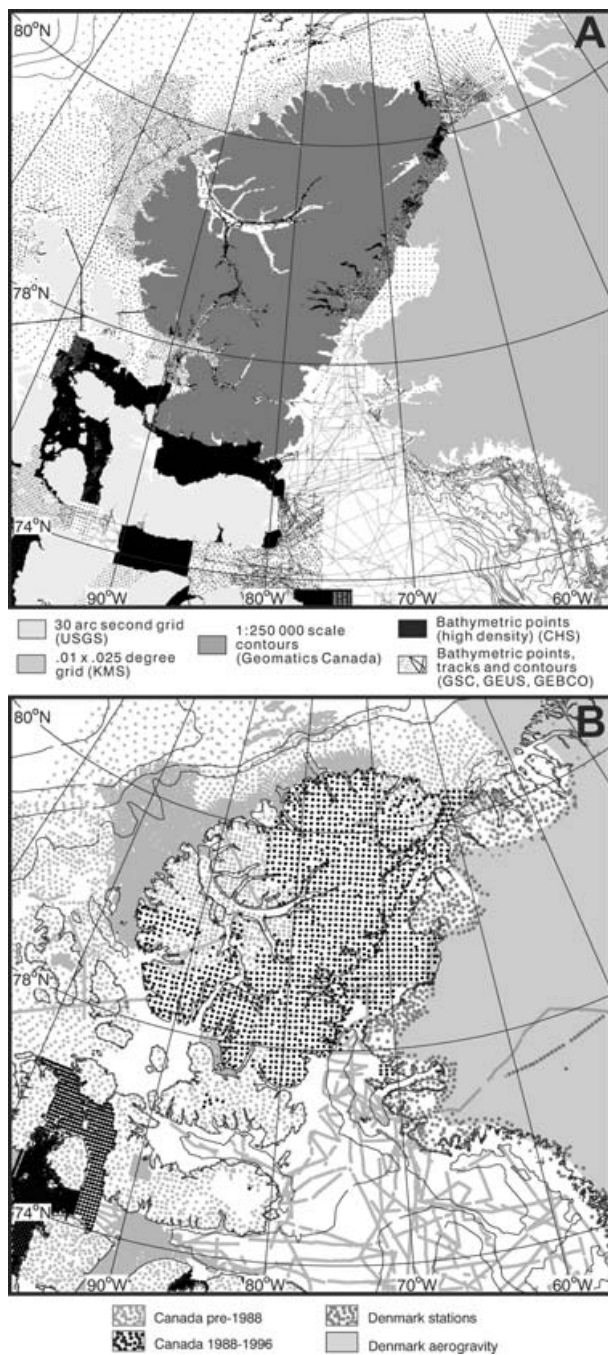
Figure 6. (a) Physiography data distribution; topographic and bathymetric data were compiled and combined to produce a 1 km grid for the Innuitian Region as part of the 'Canada–Greenland Map Series' (Oakey *et al.* 2001b). The data were regridded to 5 km resolution for gravity calculations presented in this paper. (b) Gravity data distribution. Gravity station, aerogravity and shipborne data from Canadian and Danish sources were assembled to produce a 5 km grid for the Innuitian Region. New station data incorporated in this compilation are shown as black dots.

The map (Fig. 5) shows a vast glacially dominated mountainous region with elevations on northern Ellesmere Island exceeding 2500 m, making this one of Canada'.s highest mountain ranges. Several seaward extensions of deep glacial drainage features (<600 m) are noted (Peary Channel, Nansen Sound, Lincoln Sea, Smith Sound, Inglefield Bay, Jones Sound and Lancaster Sound). Some of these drainage features have associated submerged marginal deltas, such

as Nansen Sound, and were a significant control over the Pleistocene and Quaternary evolution of the region. The amount of influence geological structures had on the geometry of these drainage features is largely unknown. Two deep-water regions (below 2000 m) are the Arctic Ocean and Baffin Bay. In the Arctic Ocean, the Alpha Ridge separates the Canada Basin from the Makarov Basin. Low data density in these areas significantly decreases the resolution of the bathymetric surface.

Ice covered areas over Canada (Grantland Ice Field, Agassiz Ice Cap, Prince of Wales Ice Field, Muller Ice Cap and Devon Ice Cap) are a mix of both broad featureless topography where ice is thick, and highly textured topography, where thinner ice reflects the fabric of the underlying bedrock. On Greenland, several ice tongues (Humbolt Glacier and Petermann Glacier) extend from the vast Greenland Inland Ice and reach the ocean. For subsequent analysis, it was also important to quantify the topography of the study area in the absence of the overlying ice bodies (as seen on Fig. 5), which reach a maximum thickness of 2400 m. Fig. 7a shows ice thickness distribution within the study area and Fig. 7b shows the resulting 'sub-ice' topography (ice thickness subtracted from topographic surface). The effects are greatest in Greenland, near the periphery of the main area of interest, and minor in Canada where the maximum ice thickness rarely exceeds 500m except the Devon Ice Cap, which has a maximum value (in the grid) of ∼800 m.

3.2 Sedimentary cover

A map of Mesozoic–Cenozoic sedimentary thickness in the study area, compiled from a number of sources, is shown in Fig. 8. There is considerable variation in the degree of detail of the information used in making this figure, as outlined in Fig. 9a. The data sources used for the Northern Baffin Bay, Lancaster Sound and KB were from industry maps, filed with the Canadian National Energy Board (see Appendix A). Since all of the industry maps were expressed as two-way traveltime (TWTT) below sea level, the time offset corresponding to the bathymetry shown in Fig. 5 was first removed to compute sediment thickness (in TWTT), using the water velocity of 1463 m s^{-1}. To convert the TWTT sediment thickness compilation to depth, an appropriate velocity model was developed, using sonobuoy refraction data from industry sources (Baffin Bay Petroleum Ltd., see Appendix A) and Keen *et al.* (1972), in the mouth of Lancaster Sound (Fig. 9b). The sonobuoy velocity measurements were not based on reversed lines and, therefore, the overall variability is fairly high due to localized geometry, and some of the largest data outliers were ignored. The individual velocity-depth curves shown in Fig. 10 were used to define an averaged velocity structure for depth conversion of the maps. The sediment velocity profiles start at 2000 m s^{-1} at the seabed and increase linearly to 3800 m s^{-1} at 2500 m. Below this depth, sediment velocity does not increase significantly. Compared with velocity profiles of 'typical' marine sediments (Ludwig *et al.* 1970), the observed sediment velocities in northern Baffin Bay region are unusually high for equivalent depths. There are two possible explanations: (1) abnormally high consolidation of the sediments in Baffin Bay or (2) a regional uplift which allowed the erosion of younger less consolidated sediments.

The sedimentary cover within northern Baffin Bay and Nares Strait can be broadly divided into rift-related basins overlying continental crust and a deep central basin over the oceanic crust of Baffin Bay. Sedimentary thickness values over the oceanic crust in central Baffin Bay exceed 9 km and are based on sonobuoy refraction seismic data (Jackson *et al.* 1977). Wide-angle refraction data over northern Baffin Bay (Reid & Jackson 1997) identify the location
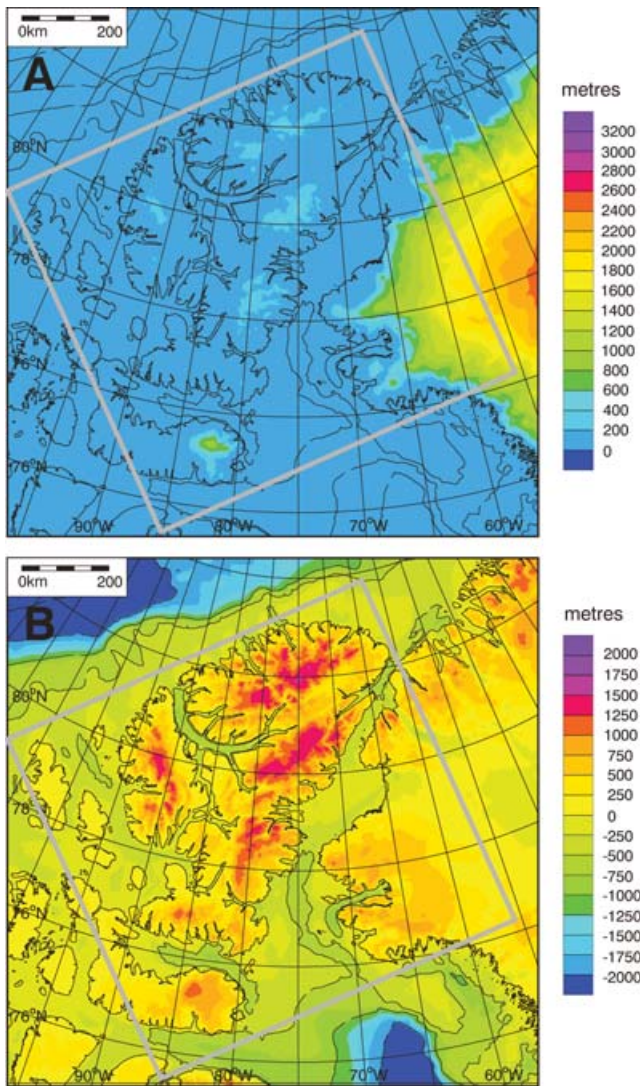
Figure 7. (a) Present ice thickness in the study area, from Bamber *et al.* (2001a, b) for Greenland and from spot elevations of ice thickness (Koerner 1977) and ice-edge polygons (Digital Chart of the World, 1992) for Canada. (b) The 'sub-ice' topographic surface in the study area by subtracting ice thickness in A from physiography in Fig. 5. The grey box shows the area of the isostatic admittance analysis (Section 4.4).

of the continent–ocean boundary (COB) seawards of the BB with a sedimentary thickness of 12 km. These limited observations have been used to constrain the extrapolated sedimentary thickness values from the more detailed industry mapping along the margins.

Sediment thickness values within the Melville Bay Graben have been produced from a combination of maps and cross-sections published by Whittaker & Hamann (1995). The 'zero-thickness' contours are defined by the inner and outer subbasin polygons, and the cross-sections provide reasonable constraints of the sediment thickness for key locations. The Melville Bay Ridge separates the inner MBG from the outer Kivioq Basin. Both basins have thicker subbasins in the south and structurally divided from shallower subbasins in the north. The inner Melville Graben dips westwards, and is truncated against a steeply dipping fault along the Melville Bay Ridge. Maximum sediment thickness is over 7 km in the south and 5 km in the north. Within the Kivioq Basin, sedimentary thickness is between 4 and 5 km.

Narrow NW–SE oriented elongated basins occur west of the Melville Bay Graben. The N–S oriented Carey Basin (CB) is a moderately deep basin with ∼5 km of structurally deformed strata. North of CB is the NW–SE oriented North Water Basin (NWB). Old exploration seismic profiling over the NWB suggested ∼5 km of low-velocity strata but are not compatible with newer seismic data, which indicate only about 3 km (Neben *et al.* 2006). The Glacier Basin (GB) is a narrow N–S oriented basin with only ∼1 km of low velocity strata. Within Kane Basin (KB), the shallow Franklin Pierce Basin (FPB) is structurally bounded to the west by the Eurekan Frontal Thrust.

The Lancaster Basin (LB) is a half graben, with northward dipping strata bounded by the Parry Channel Fault, with over 5 km of strata in two localized depocentres. The Lancaster Basin is separated from the Bylot Basin (BB) by the NW–SE oriented Hope Structure Ridge, named after and industry seismic line (Baffin Bay Petroleum Ltd., Appendix A). The Lady Anne Basin (LAB) contains over 4 km of strata and is bounded to the south by another NW–SE oriented basement ridge (the Philpots Ridge, Rice & Shade 1982).

The least detailed areas are the Arctic Ocean and the Sverdrup Basin, where very generalized regional-scale maps of sedimentary thickness (in km) were used (Jackson & Oakey 1990; Embry 1991). Off the Canadian Arctic margin, within the Canada Basin, sediments are thicker than 12 km, thinning to less than 2 km over Alpha Ridge. Within the Lincoln Sea, two elongated basins with over 6 km of strata are separated by a structural high with less than 4 km of sediments. The Sverdrup Basin contains more than 8 km of Mesozoic strata. It is separated from Canada Basin by a structural high, called the Sverdrup Rim, that parallels the present continental margin.

3.3 Gravity field

The gravity data used in this study (Fig. 11) are from Oakey *et al.* (2001a), compiled from shipborne, airborne, and both onshore and sea-ice station gravity observations. Station data for Canada and its margins were provided by the Canadian Geophysical Data Centre (2000) and includes approximately 2000 previously unpublished new gravity stations collected in 1995 over Axel Heiberg Island, Ellesmere Island and Kane Basin (Maye 1995; Hearty *et al.* 1996). Station data and gridded aerogravity data over Greenland and its margins were provided by the Danish National Survey and Cadastre (1998). Data sources are shown in Fig. 6a. The average spacing of the gravity observations over land is ∼5 km and between 5 and 30 km for the ships tracks.

The gravity field for the Innuitian Region (marine free-air and onshore Bouguer anomalies) is displayed in Fig. 11 along with a simplified overlay of some of the major structural elements and features interpreted from the gravity data, discussed later. The Bouguer correction for onshore areas assumed a crustal rock density of 2670 kg m^{-3}. For measurements on lakes and glaciers, densities of 1000 and 900 kg m^{-3} were used for water and ice, respectively. Terrain corrections were applied in some coastal regions where measurements were made adjacent to fjords.

A 'complete' Bouguer anomaly field (Fig. 12) was calculated by reducing the marine free-air anomalies using the bathymetric data shown in Fig. 5. This was done by replacing the water column with crustal density rocks using an algorithm in which the water layer was simulated by millions of cubes (Oakey 2005), based on the polynomial expansion of the gravitational effect of a 3-D cube derived by Nady (1966). This correction eliminates the artificial gravity lows (in the free-air anomaly field) that are associated with deeply scoured shelf areas and improves onshore–offshore
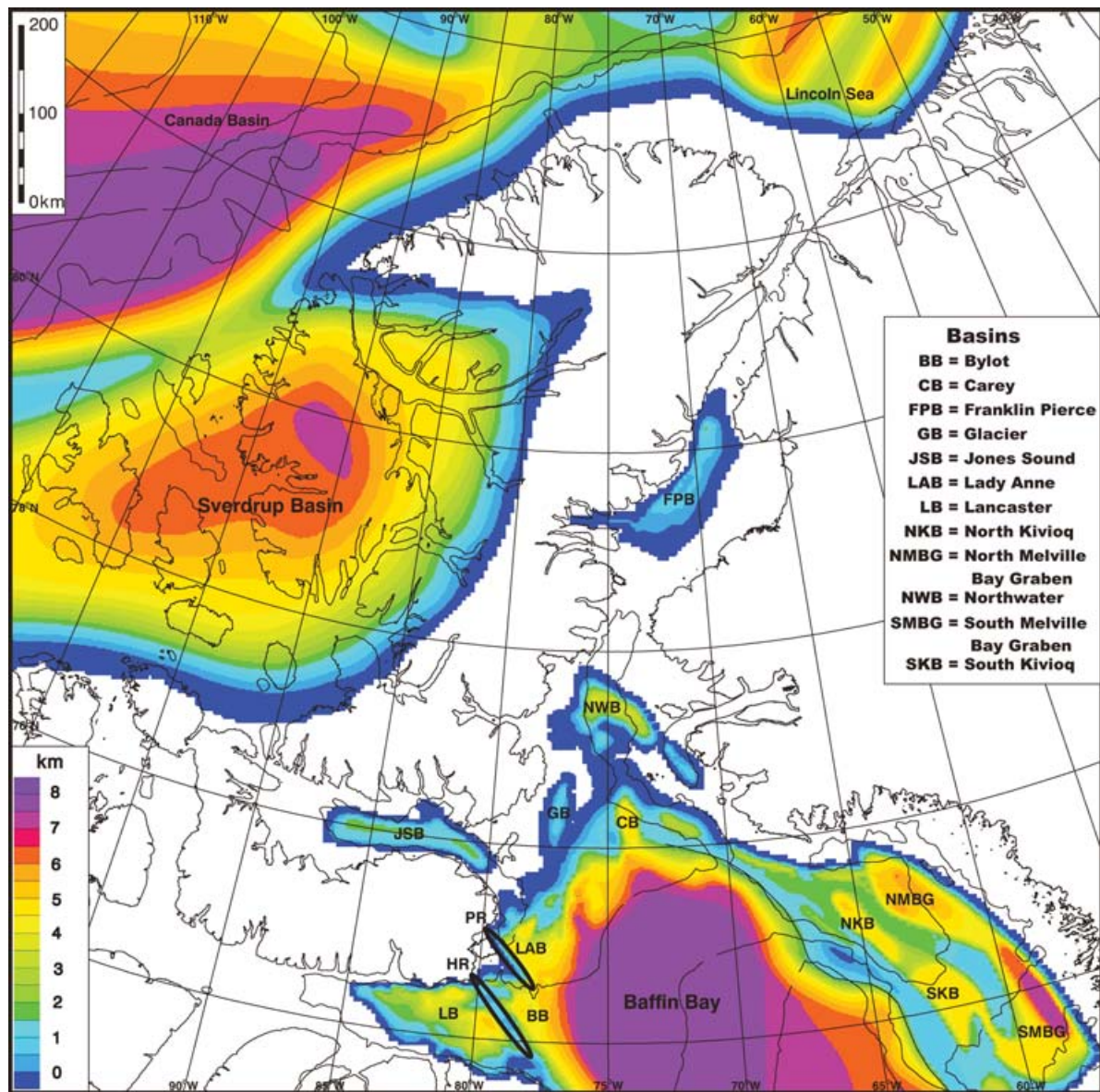
Figure 8. Sedimentary thickness in the study area, produced on a 5 km grid, as discussed in the text from sources shown in Fig. 9a. Two structural features mentioned in the text are shown with narrow ovals: the Philpots Ridge (PR) and the Hope-Structure Ridge (HR).

correlation of geologically related features. This correction also minimizes the gravity highs associated with the geometry of the shelf break; however, it results in a large positive gravity anomaly over the deep ocean basins where the Moho depths are shallow.

Finally, the compiled Mesozoic–Cenozoic sediment thickness data have been used to calculate a 'crustal Bouguer' (CB) anomaly (Fig. 13) that corrects for the gravitational effects of low density strata within the basins. This correction tends to amplify gravity anomalies related to crustal thinning beneath sedimentary basins. The residual 'crustal' anomaly is, in principle, a combination of variable crustal thickness (i.e. variable Moho depth) and density heterogeneities within the crust. Obviously, it may also incorporate errors in the water and (especially) sedimentary layer models used in its construction. The two-layer density model used for this correction was based on an empirical relationship between sediment velocity and density (Barton 1986) and the velocity model defined by the sonobuoy data shown in Fig. 10. The density applied to the first 2 km of sediments was 2200 kg m^{-3} and for the next 3 km

a density of 2400 kg m^{-3} was applied. It has been assumed that sediments deeper than 5 km are sufficiently compacted so that their density is close to average upper crustal density. Although density data exist from exploration wells within the Sverdrup Basin, these were not available for this study. No compensation has been made for either Mesoproterozoic Thule Supergroup sequences or strata of the Palaeozoic Franklinian margin, due partially to a lack of thickness data, and partially to the high (near-crustal) densities observed from samples within the balanced cross-section shown in Fig. 3.

4 ANALYSIS OF THE GRAVITY FIELD OF THE INNUITIAN REGION

4.1 Overview

The gravity field, in any of the versions in which it was presented for the study area (Figs 11–13), can be readily correlated with tectonic province, defined as: (1) areas of oceanic or thinned continental crust
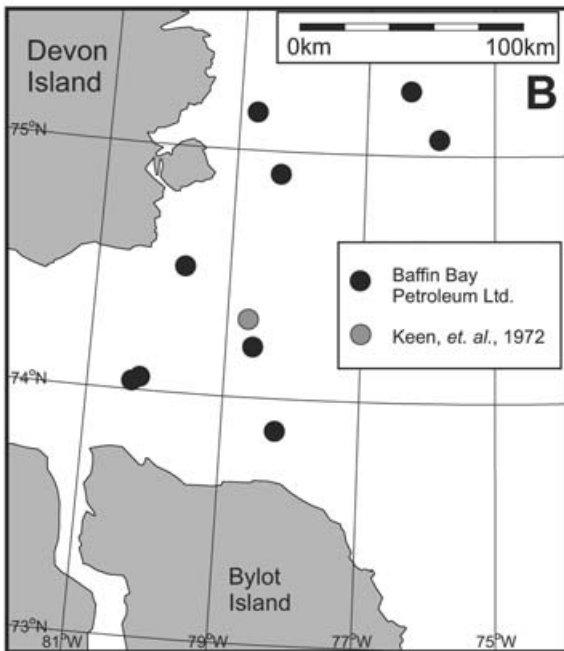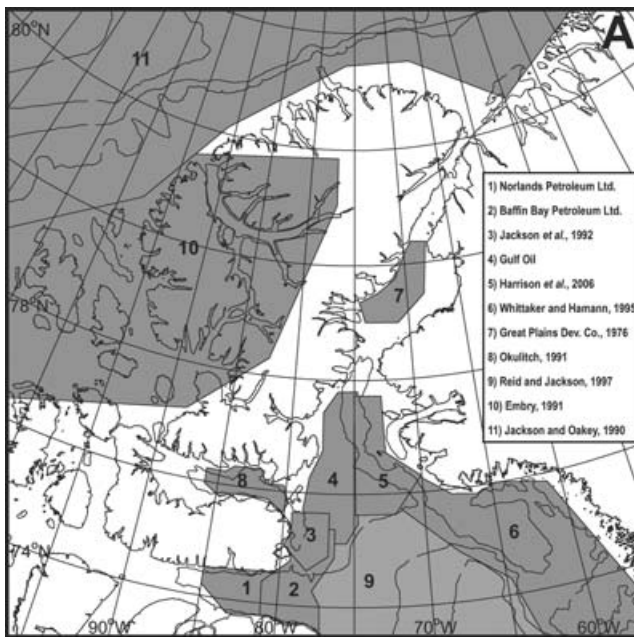
Figure 9. (a) Data sources used in constructing the sedimentary thickness map shown in Fig. 8. Details of industrial sources are listed in Appendix A. (b) Locations of sonobuoy refraction data used to convert the two-way travel time compilation of sediment thickness to depth in Fig. 8.

Figure 10. The 1-D velocity structure at sonobuoy locations shown in Fig. 9b (thin black lines) 'stacked' to define an average velocity-depth curve (solid grey line, increasing linearly from 2000 m s^{-1} at the seabed to 3800 m s^{-1} at 2500 m and constant at greater depths) that was used to convert TWTT to depth in areas 1–8 (Fig. 9a). Also shown is the velocity–density curve (dotted line with data scatter shown in grey) by Barton (1986). The densities used for calculating the 'crustal' Bouguer anomaly (Section 3.3) are 2200 kg m^{-3} for layer 1 (2 km thickness) and 2400 kg m^{-3} for layer 2 (2–5 km).

(including the continental margins of the Arctic Ocean and Baffin Bay and the Sverdrup Basin); (2) areas with crust involved in and possibly thickened as a result of Eurekan compressional tectonics and (3) the preserved cratonic continental areas of Greeenland and adjacent parts of Canada.

The offshore parts of the study area display the greatest variations between gravity maps. This is because the modifications to the initial map (Fig. 11) involve corrections for the water layer (Fig. 12) and for the sediment layer (Fig. 13), with both layers being most prominent in the offshore, continental margin areas. The prominent positive
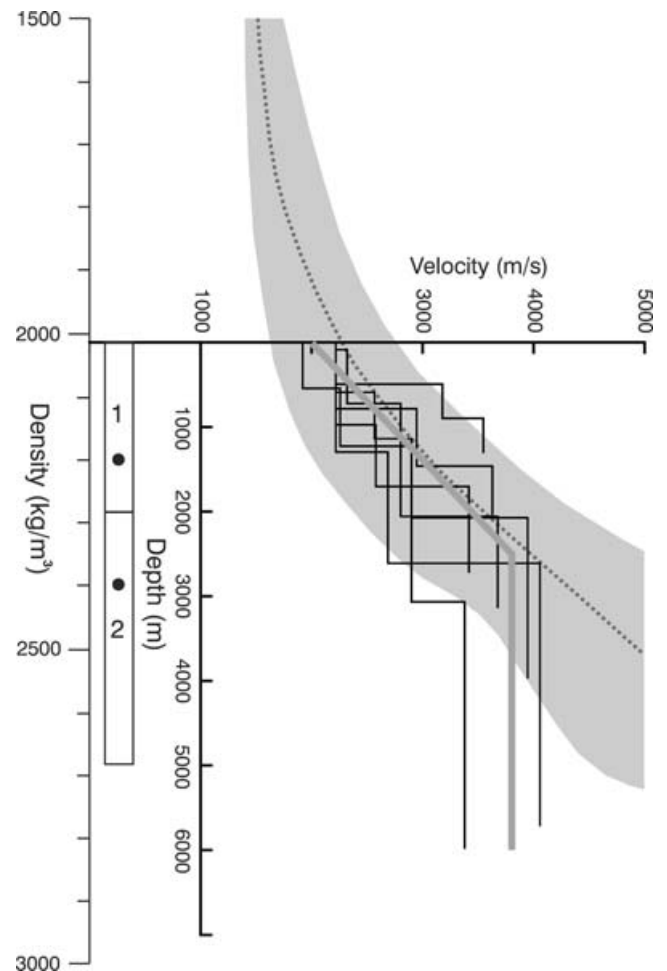
free-air anomaly trend following the shelf break (∼500m) in Fig. 11 is not seen in Fig. 13, where continent–ocean edge effects and the gravitational signature of thick, prograded sediments (Keen *et al.* 1990; Forsyth *et al.* 1998) have been removed. The COB roughly corresponds with the 160 mGal contour in the Crustal Bouguer (CB) anomaly field (Fig. 13), calibrated by one seismic refraction profile (heavy black line labelled F94; Forsyth *et al.* 1994) in the Lincoln Sea. The same definition has been applied in Baffin Bay, where it corresponds well with the position of the COB determined by Reid & Jackson's (1997) refraction data.

Some of large free-air gravity lows over with deep-water channels, such as Inglefield Bay (IB; Fig. 5), are eliminated by the Bouguer correction (Fig. 11 versus Figs 12 and 13), indicating that these are associated with deep ice scouring of shelf areas that are not isostatically compensated. The Jones Sound gravity low (JSL) has not been eliminated, although its amplitude is reduced. In Lancaster Sound, not only has the gravity low (LSL) been eliminated, but a significant seaward continuation and amplification of the coastal gravity high (LSH) is revealed. The CB anomaly (Fig. 13) locally
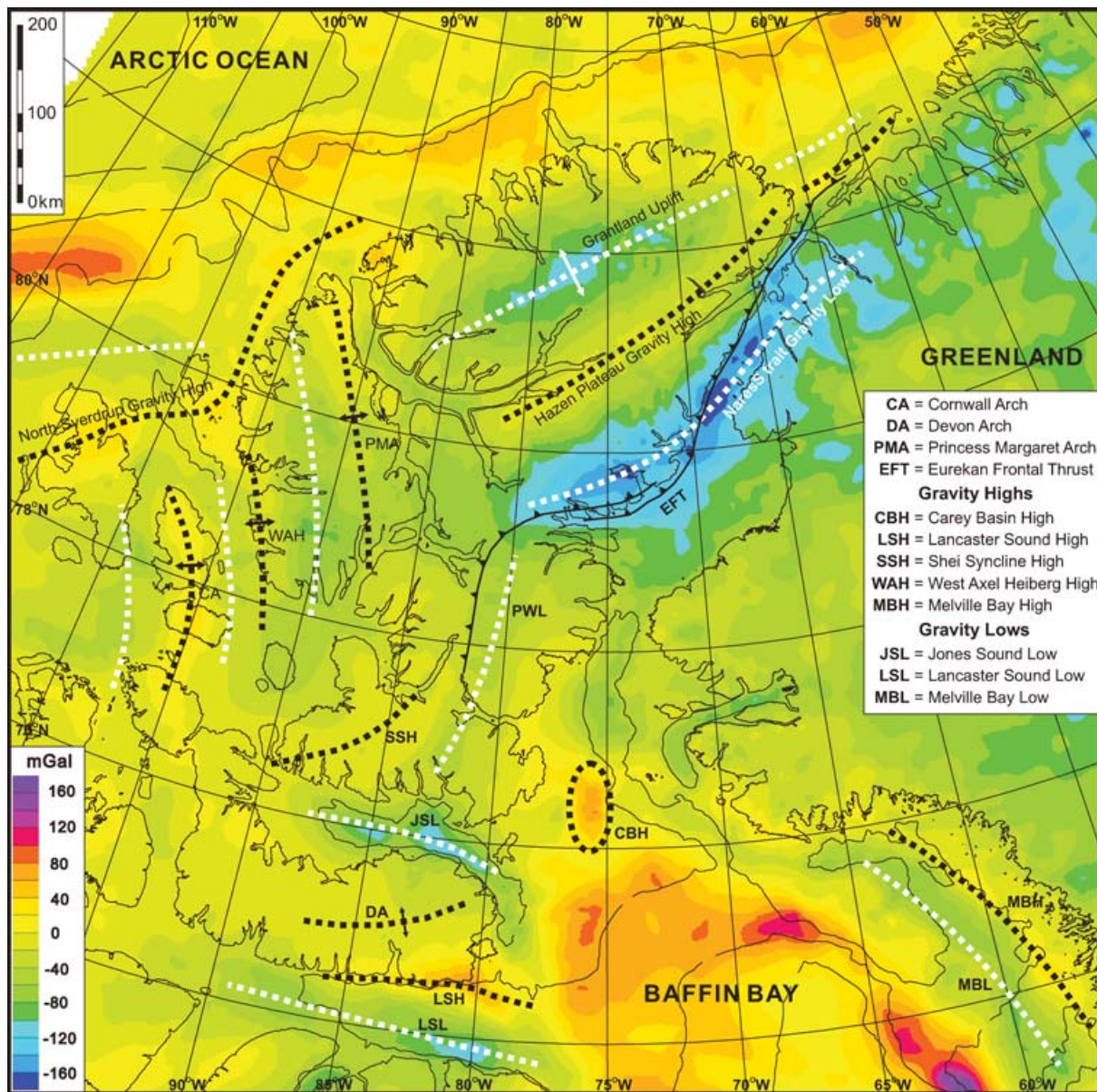
Figure 11. Marine free-air gravity and onshore Bouguer anomaly map, from Oakey *et al.* (2001a). The Bouguer correction for onshore areas assumed a rock density of 2670 kg m^{-3}; for measurements on lakes and glaciers, densities of 1000 and 900 kg m^{-3} were used for water and ice, respectively. Terrain corrections were applied in some coastal regions where measurements were made adjacent to fjords. The axes of linear gravity highs and lows discussed in the text are also shown (dashed black and white lines, respectively). Also shown are the Eurekan Frontal Thrust (EFT) in northern Nares Strait (Harrison 2006) and the Devon Arch (DA).

exceeds 120 mGal and is imaged as a triangular feature, axially symmetric about the central gravity high. The axis of Lancaster Basin is coincident with a landwards extrapolation of the extinct (Eocene) spreading axis within Baffin Bay and is interpreted to be a failed rift-arm of this spreading system. Similarly, the large positive, isolated, Carey Basin High (CBH) anomaly (>60 mGal in Fig. 13) north of Baffin Bay is also reportedly associated with significant Moho shallowing (Jackson & Reid 1994). In Melville Bay, on the Greenland shelf, the negative CB anomaly (MBL; Fig. 13) associated with the main depocentre of the MBG (Fig. 2) is subdued, though not eliminated, compared with the free-air anomaly (Fig. 11), and a residual positive trend probably indicates crustal thinning beneath this graben, slightly offset relative to the main shelf parallel depocentre.

Onshore regions in the study area, including the Canadian Arctic Archipelago, are characterized by CB gravity values that are negative or less positive than those of the oceanic or suboceanic regions. This is particularly true for Greenland where the continental crust is, probably, generally thicker than for the Canadian Arctic Archipelago, based on limited receiver function estimates of crustal thickness: >37 km (Dahl-Jensen *et al.* 2003) and ∼34 km (Darbyshire 2003), respectively.

Within the SID (Section 2.3; Fig. 2), the CA and PMA arches are characterized by relative gravity highs. These structures were previously interpreted to correspond with the crests of crustal-scale folds, involving Moho uplift (Stephenson & Ricketts 1990). A third N–S oriented linear gravity high can be identified along the western edge of Axel Heiberg Island (WAH), approximately equidistant
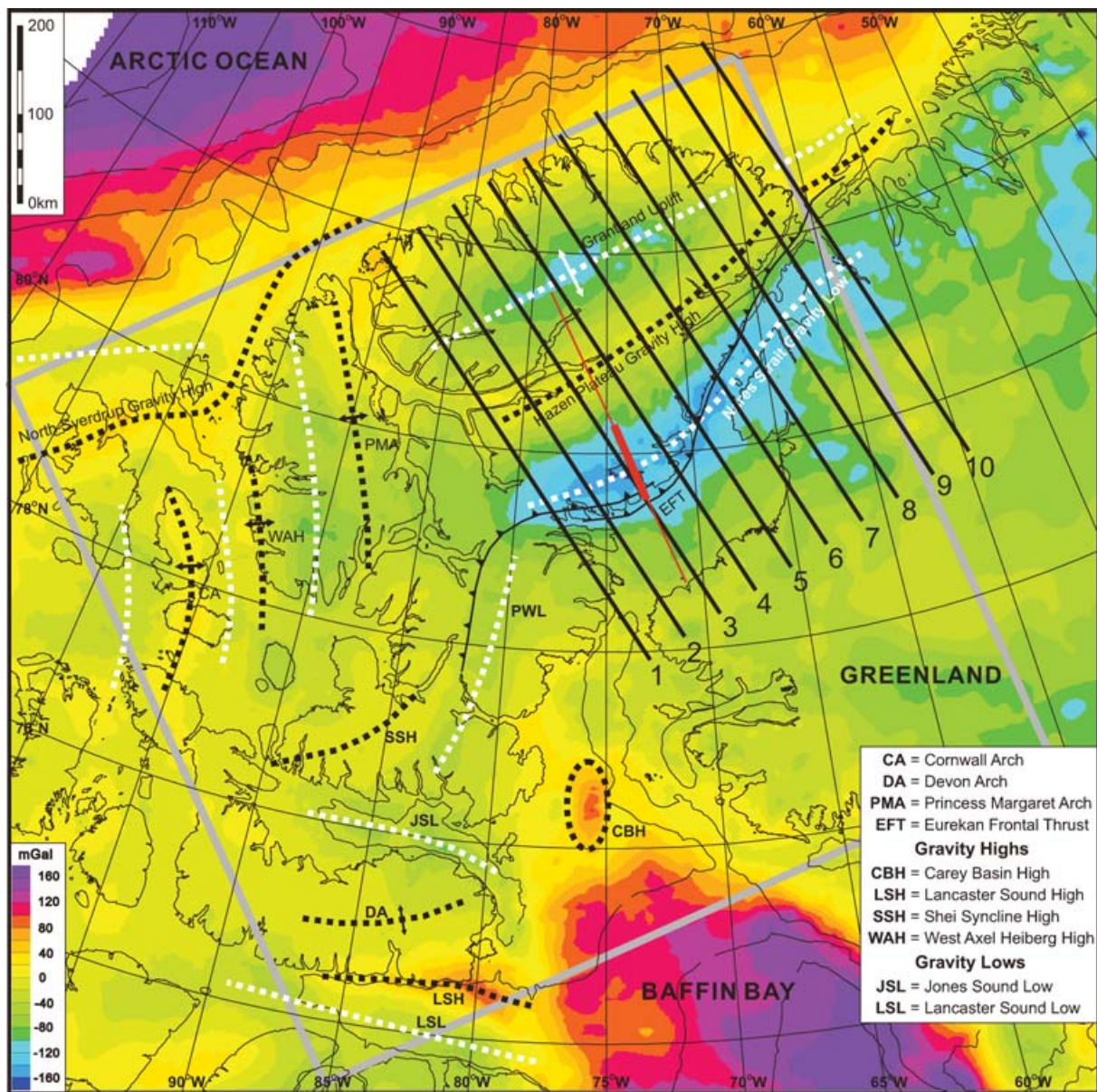
Figure 12. Bouguer anomaly map of the study area, in which the water density of 1030 kg m^{-3} was substituted with a crustal rock density of 2670 kg m^{-3} based on bathymetry seen in Fig. 5. Gravity and geological features mentioned in the text are shown as for Fig. 11. In addition, the locations of 10 profiles (including a modelled profile in red along the geological cross-section seen in Fig. 4) and the outline of the area used for the isostatic admittance analysis (grey box) discussed later (sections 4.3 and 4.4, respectively) are also included.

between the CA and PMA, and it likely represents a previously unrecognized crustal arch. The spacing between these three features is ~100 km, similar in wavelength to the Moho topography suggested by low-resolution refraction seismic data west of the CA (Forsyth *et al.* 1979).

An anomalous trend in the Bouguer gravity field (Fig. 11), comprising a number of isolated anomalies from northern Ellef Ringnes Island eastwards to the southern edge of Meighen Island and northwards off the coast of Axel Heiberg Island (see Fig. 5 for geographic locations), is more continuous and of significantly greater amplitude in the CB field (Fig. 13). It is referred to as the North Sverdrup Gravity High (NSGH) and is likely related to mafic sills and dykes that intrude Sverdrup Basin strata in this region. However, it is possible that much of the amplification of the NSGH may be artificial, related to the poor resolution (smaller mappable scale) of the sed-

iment thickness contours introduced for the Sverdrup Basin (i.e. Fig. 8).

Within the Northern Ellesmere Domain (Section 2.3; Fig. 2), the Grantland Uplift (GU) corresponds to the broad NE oriented GU gravity low (GUGL), attributed to isostatically compensated thickened crust (Stephenson & Ricketts 1990). South of the GUGL is the NE oriented linear Hazen Plateau Gravity High (HPGH) that extends from the head of Nansen Sound to the Lincoln Sea (see Fig. 5). The HPGH coincides with the inferred source of the 'alert geomagnetic anomaly' (Niblett *et al.* 1974), which was attributed to an elongated conductive body within the crust. The GU and the HPGH can be tentatively linked to unnamed collinear gravity lows and highs in the Lincoln Sea, especially as portrayed in Fig. 13.

Outside of oceanic regions, the most significant feature of the gravity field of the Innuitian Region is the NSGL, a large negative
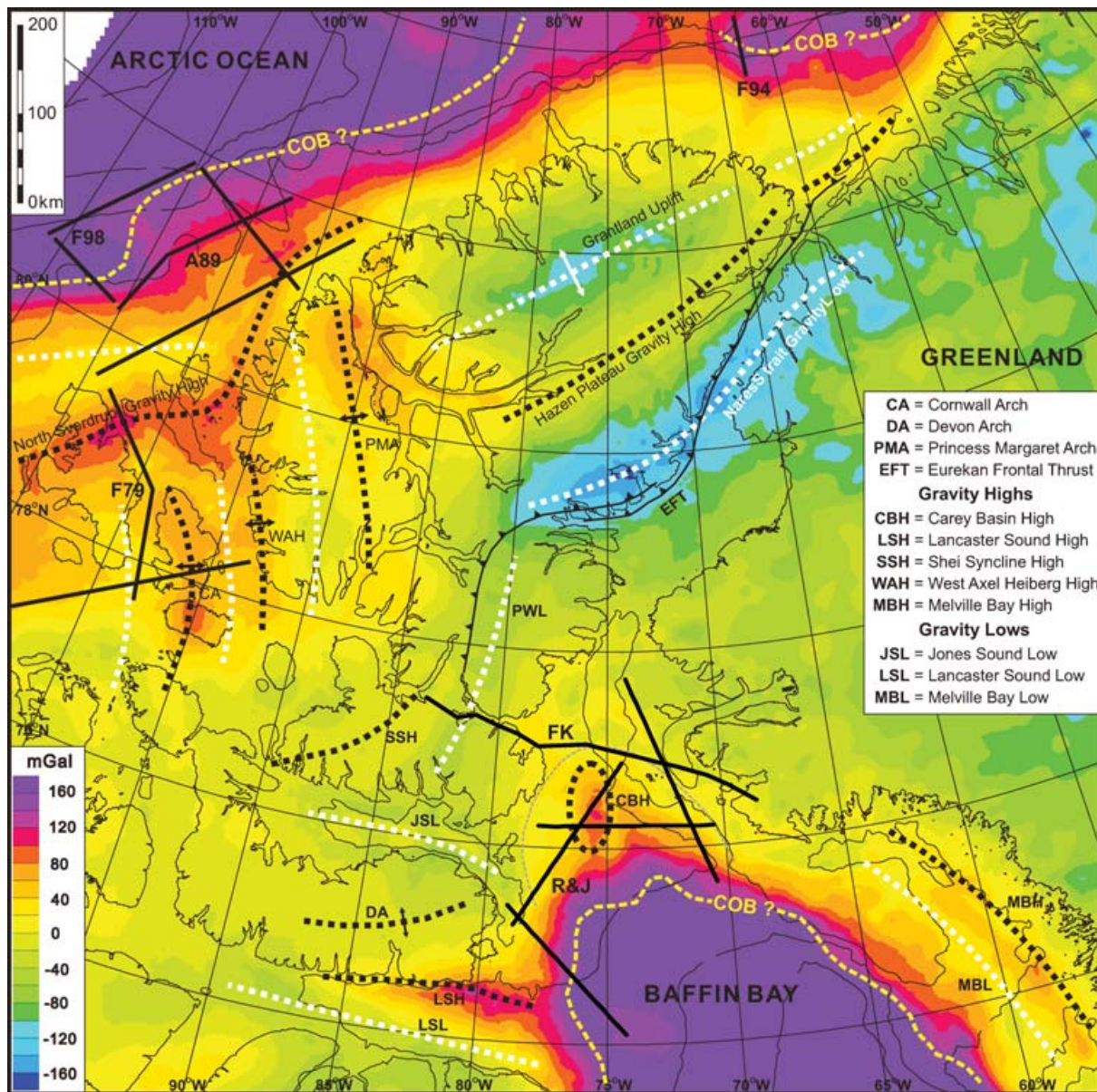
Figure 13. 'Crustal Bouguer' anomaly map of the study area, in which the gravitational effects of sediments (as defined in Fig. 8) have been removed, as described in the text (Section 3.3). Gravity and geological features mentioned in the text are shown as for Fig. 11. The minimum seaward extent of the continent–ocean boundary (COB) is shown with a dashed yellow line. Also shown are the locations of refraction lines in Lincoln Sea (F94—Forsyth *et al.* 1994); Sverdrup Basin and adjacent continental margin (F79—Forsyth *et al.* 1979; A89—Asudeh *et al.* 1989; F98—Forsyth *et al.* 1999); and northern Baffin Bay (R&J—Jackson & Reid 1994; Reid & Jackson 1997; FK—Funck *et al.* 2006) as well as locations where receiver function derived estimates of Moho depth are available: AL, Alert; EU, Eureka; GF, Grise Fiord; RB, Resolute Bay (Darbyshire 2003); TH, Thule (Dahl-Jensen *et al.* 2003).

anomaly that extends from Ellesmere Island, across KB, KC, and continues across North Greenland. The southernmost end of this feature was identified by Jackson & Koppen (1985) from a single gravity traverse across Nares Strait and attributed to severe crustal thickening from continental collision during the Eurekan Orogeny. However, the frontal thrust of the Eurekan Orogen (Harrison *et al.* 2006), labelled EFT in Figs 11–13, is oblique to the trend of the NSGL. This is demonstrated in Fig. 14 where ten parallel profiles crossing the NSGL are aligned according to the crossing position of the EFT. The widths of the NSGL, as well as the associated HPGH and GUGL, are quite uniform along strike, with the NSGL approximately 150 km, the HPGH between 80 and 100 km, and the GUGL approximately 80 km. For lines 9 and 10, the EFT passes

through the HPGH, well to the north of the NSGL. Between lines 7 and 8 the EFT crosses the boundary between the HPGH and the NSGL. For lines 1 to 6, the EFT clearly passes obliquely through the NSGL. This cross-cutting geometry suggests that the source of the NSGL is not primarily the result of plate convergence (and crustal thickening) during Eurekan orogenesis. Rather, the NSGL low closely follows the distribution of Paleozoic Franklinian shelf and slope sequences and it is interpreted to be the signature of the near-surface geology, dominated by sedimentary successions of the Palaeozoic continental margin.

Although the NSGL can only be traced as far south as 79°N, a lower amplitude NS oriented gravity low (~ -40 mGal), called the Prince of Wales Low (PWL), lies along the western edge of
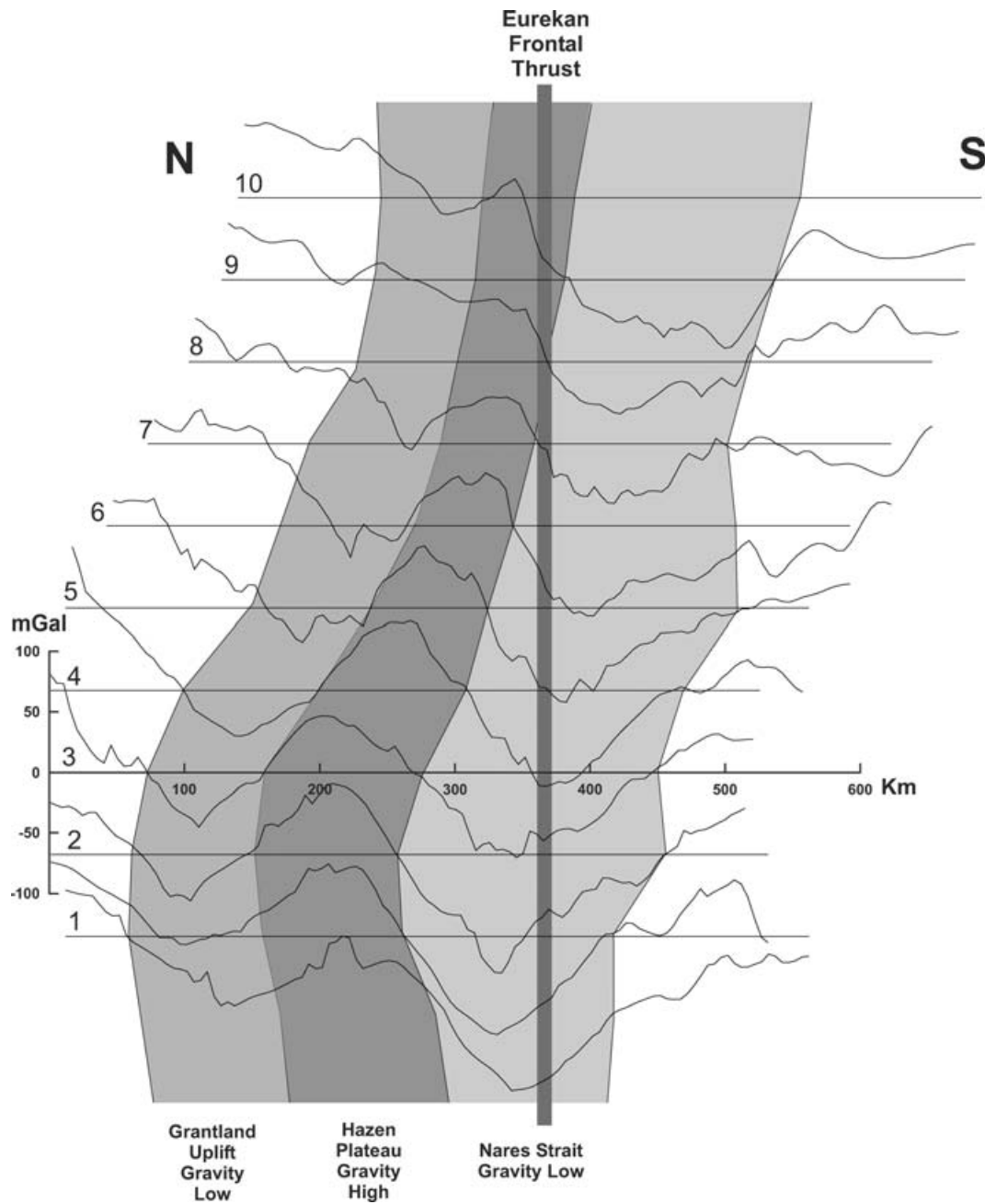
Figure 14. Bouguer gravity Profiles across the NSGL, aligned to where they cross the Eurekan Frontal Thrust. The extent of the NSGL as well as those of the Hazen Plateau high and the Grantland Uplift low are depicted with different shades of grey.

the Prince of Wales Icefield (see Fig. 5). This feature can be traced south to Jones Sound and roughly correlates with the Arctic Platform sequences along the western edge of the Archaean Craton (see Fig. 2). The low amplitude linear Shei Syncline High (SSH) runs along the western edge of the PWL, coinciding approximately with shelf province strata within the Central Ellesmere Domain (Section 2.3; Fig. 2).

4.2 Crustal affinity in the innuitian region

4.2.1 Depth-to-Moho from gravity field inversion

The CB anomaly (Fig. 13) was inverted to determine Moho depth using a technique developed by Jacob Verhoef (Personal Commu-

nication, 1990) at the University of Utrecht using Parker's (1972) method, which assumes that the crustal density is uniform and that the gravity field is generated by a single density contrast across the Moho boundary surface. The inversion method requires filtering to remove the short wavelength anomalies, since these features are not generated at Moho depths and are amplified by downwards continuation (Pilkington & Crossley 1986, Marillier & Verhoef 1989). Numerous inverse models were computed using ranges of low-pass cut-off wavelength (20–200 km), initial Moho depth (30–50 km), and density contrast across the Moho (400–600 kg m^{-3}). The solution shown in Fig. 15 is based on a cut-off wavelength of 62 km, an average (initial) Moho depth of 35 km and a density contrast of 500 kg m^{-3}. This solution was chosen because it provided the best qualitative fit with the available seismic data.
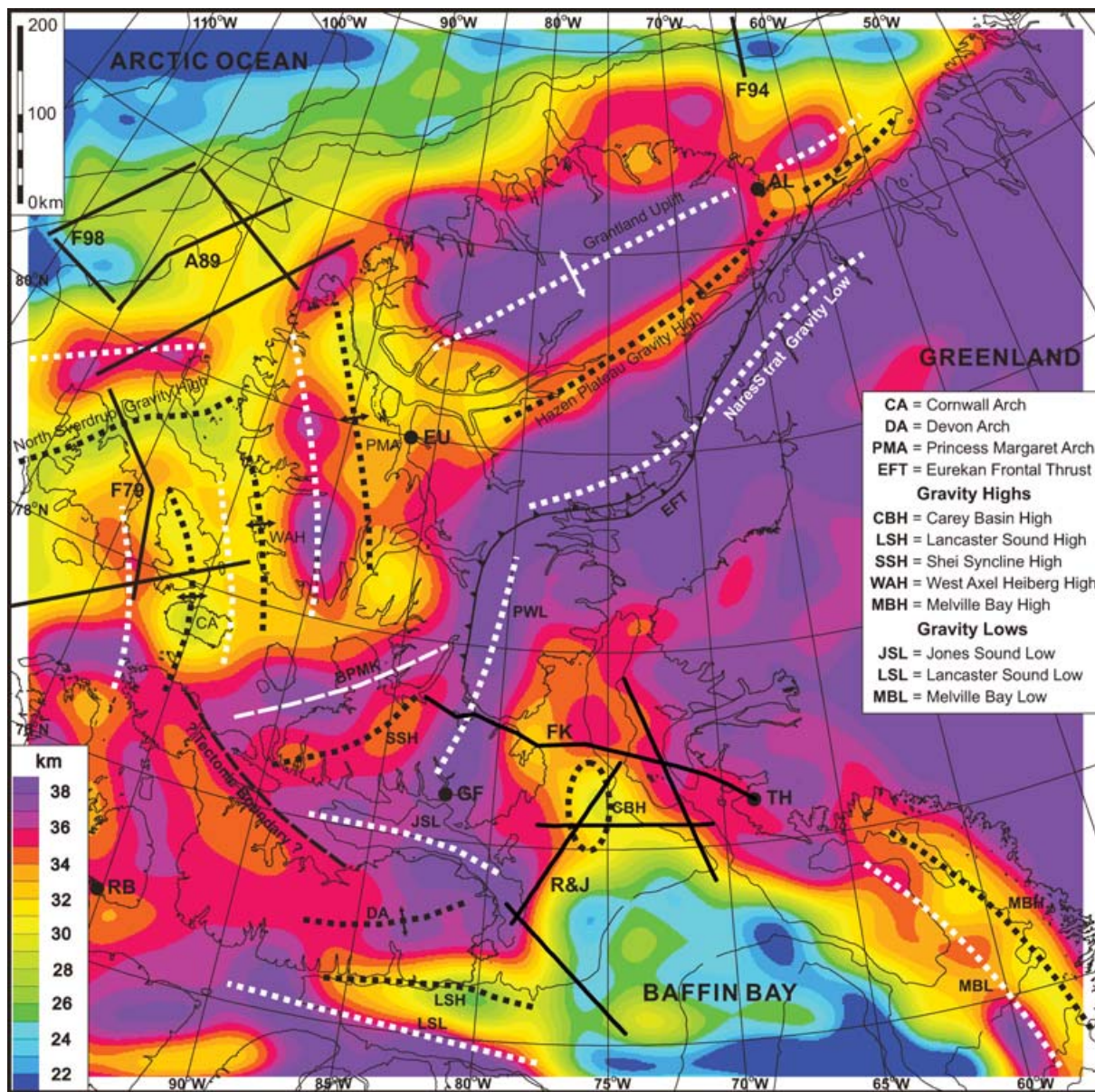
Figure 15. Depth-to-Moho in the study area from the inversion of the 'crustal Bouguer' anomaly in Fig. 13. The axes of the main gravity highs and lows discussed in the text are shown (dotted black and white lines respectively) as well as the position of the Eurekan Frontal Thrust (EFT), the Bjorne Peninsula Moho 'keel' (BPMK; white dashed line), and an inferred tectonic boundary terminating the western end of the Shei Syncline and BPMK. Locations of refraction profiles and receiver function stations as in Fig. 13.

The gravity inversion Moho is uniformly deep over Greenland, generally over 40 km, which is compatible with the limited refraction results of ~36 km at the eastern end of line FK (Funck *et al.* 2006). A depth of ~36 km in Fig. 15 at Thule (TH) compares with a receiver function depth of ~37 km from Dahl-Jensen *et al.* (2003). The Greenland relatively deep Moho merges with that of NSGL area, which indicates a 150 km wide, 40 km deep Moho structure, running from northern Greenland across Nares Strait and onshore Ellesmere Island. This structure changes orientation and continues to the south following the PWL, crossing Jones Sound onto Devon Island, west and northwest of Baffin Bay. The width of this southern zone is <80 km wide with Moho depths between 36 and 38 km. These are in agreement with the refraction results of ~37 km at the western end of line FK (Funck *et al.* 2006) and only slightly

higher than the receiver-function depth of ~34 km at Grise Fiord (GF)(Darbyshire 2003).

Beneath central and western Devon Island and surrounding areas, the inversion Moho depths are generally between 34 and 36 km, with isolated highs and lows. The receiver function depth of ~35 km at Resolute Bay (RB)(Darbyshire 2003) is the same as the inversion result. West of the PWL, the inversion Moho depths associated with the Shei Syncline gravity high (SSH) are ~35 km with its northern edge bounded by a Moho 'keel' (~38 km) beneath the Bjorne Peninsula (BPMK). A linear termination at the western end of the SSH and BPMK can be traced along the northeastern coast of Devon Island (dashed line). This lineation is coincident with the Grinnell Range—Douro Range fold and thrust belt (Mayr *et al.* 1998) and suggests a major crustal-scale tectonic boundary.

Further to the southwest, a single receiver-function analysis indicates a Moho depth at Resolute Bay (RB) of 35 km (Darbyshire 2003), which is also the value derived in the gravity inversion.

Moho depth beneath the GU on northern Ellesmere Island and its prolongation into the Lincoln Sea exceed 38 km. Between the GU and the NSGL, a narrow zone of anomalously shallow Moho (<34 km) occurs beneath the Hazen Plateau, also with a prolongation into the Lincoln Sea. The inversion Moho depth of ~32 km at Alert (AL) compares with the upper limit of the receiver-function depth estimate (26–32 km; Darbyshire 2003), but the receiver-function indicates a highly anisotropic crustal structure.

At Eureka (EU), within the Sverdrup Basin, the receiver function depth is poorly constrained in the range 36–44 km (Darbyshire 2003), greater than the gravity inversion depth of 33–34 km. That EU lies along the trend of the Hazen Plateau gravity high may be a factor in explaining this discrepancy. The refraction profiles lying further west in the Sverdrup Basin (F79—Forsyth *et al.* 1979) are old and of very low resolution. As mentioned earlier, the Moho undulations implied by the CA and PMA and associated structures in Fig. 15, are compatible with the refraction interpretations (indicating 4–5 km Moho relief). No receiver function data exist for this area. The shallow Moho structure corresponding with the North Sverdrup gravity high (NSGH) may be at least in part an artefact, as mentioned earlier, given the probable role of near-surface mafic intrusive rocks in generating this anomaly and the amplification of this effect in calculating the crustal Bouguer gravity field. To its north, the inversion Moho deepens to more than 35 km, correspond with the position of the 'Sverdrup Rim' defined by Embry (1991). In consideration of the 'NSGH artefact' (discussed in Section 4.1) it is possible that the axis of the Sverdrup Rim is further to the north. Gravity modelling across the Sverdrup Rim by Sobczak (1991) defined a pronounced crustal root of over 45 km in this area, significantly deeper than the present results; however, the crustal densities used by Sobczak were substantially higher, which would explain the discrepency.

Along the Arctic margin, north of the Sverdrup Basin and in the Lincoln Sea, the refraction Moho (A89—Asudeh *et al.* 1989; F94—Forsyth *et al.* 1994; F98—Forsyth *et al.* 1998) is reasonably close to the results of the gravity inversion. This is also the case over the deepwater part of northern Baffin Bay, which is presumably oceanic crust (R&J—Jackson & Reid 1994; Reid & Jackson 1997). A well defined prolongation of extremely shallow Moho, with depths of <26 km, extends from the oceanic area of Baffin Bay into Lancaster Sound. This is the shallowest solution determined for any continental area in the Innuitian region. In the area of the Carey Basin (CBH), the inversion Moho depths of 28–30 km are significantly less than those of the refraction results, which are in the range 22–24 km. Although this discrepancy suggests that the densities applied to the sediments were too high and the resulting crustal Bouguer anomaly (Fig. 13) is too low, the filter parameters used in the inversion limit the resolution of isolated detailed features. Further to the southeast, on the Greenland margin of Baffin Bay, the gravity inversion suggests that the fairly continuous Melville Bay Ridge (associated with the MBL; Fig. 15), with a fairly normal continental Moho depth of 32–36 km, separates the inner Melville Bay Graben, with a shallow Moho depth of ~30 km, from the main Baffin Bay basin.

4.2.2 Crustal thickness

Crustal thickness (Fig. 16) has been calculated by subtracting the depth-to-basement surface from the Moho depths produced by the gravity inversion. The depth-to-basement surface is defined as the sub-ice surface minus the sediment thickness values (Figs 7b and 8, respectively). High-frequency variations in the crustal thickness values were reduced by smoothing the depth-to-basement grid with a 20 km filter. Since the Moho depths are with respect to a sea level datum, and the depth-to-basement surface is both above and below sea level, the crustal thickness map provides a useful representation of the regional crustal geometry. It is important to note that this 'crustal thickness' is a combined total of the Archaean crystalline basement plus the dense strata of the Meso-Proterozoic Thule Supergroup and Proterozoic Franklinian margin sequences.

For continental areas, without Mesozoic and Cenozoic sedimentary cover, the crust is consistently 34–36 km thick. Over Greenland, crustal thickness inland of Melville Bay exceeds 40 km, suggesting that there may be several kilometres of sedimentary rocks beneath the ice sheet that have not been taken into account. Conversely, the influence of the ice load may be producing additional artefacts that have also not been accommodated in this modelling. The large crustal thickness values corresponding with the NSGL generally exceed 40 km, with a maximum thickness of >42 km along the Ellesmere Island coast, where it crosses the EFT and localized Eurekan deformation has thickened the Paleozoic strata. Continuing to the south, the crustal thickness values decrease slightly to ~38 km along the PWL, suggesting that equivalent Palaeozoic strata have been uplifted and eroded.

Crustal thickness values corresponding with the GU also exceed 42 km, more notable as an anomalous feature than from the depth-to-Moho solution, due to the contributing effect of extremely high mountains. As mentioned earlier, the GU contains remnants of the Sverdrup Basin (i.e. post-Ellesmerian) strata along a zone of extremely complex basement geology and likely represents a region of extreme Eurekan crustal thickening. The Hazen Plateau Gravity High separates the GU from the NSGL, with typical crustal thickness values of ~35 km, suggesting that little or no Eurekan deformation occurred within this zone and is consistent with it being described as a 'stable block' (Section 2.3; Fig. 2).

The Sverdrup Basin is shown in Fig. 16 as a broad region of substantially thinned crust. The northern edge of the basin is bounded by the Sverdrup Rim, which is imaged as a continuous crustal feature with thicknesses between 32 and 34 km. In the central part of the basin, the crustal thickness values have a minimum of <22 km associated with the North Sverdrup Gravity High. As mentioned earlier, there are likely uncorrected volcanic intrusives associated with this gravity anomaly, and the resulting crustal thickness values are too thin. As such, the crustal thickness within the Sverdrup Basin is more reasonably only ~24 km, corresponding with a 30% crustal thinning of 'normal' (35 km) crust. Stated in terms of the commonly used crustal 'stretching' factor β, this corresponds to a value of ~1.3. The N–S oriented gravity low over central Axel Heiberg Island corresponds with a zone of crustal thickening with values ranging from ~26 km in the north to over 30 km in the south. If this structure represents a Eurekan overprinting of the basin, then shortening was on the order of ~15% corresponding to a β of ~0.85 (i.e. thickening from 24 to 28 km). Additionally, if the GU is also a Eurekan structure that completely exhumed the original Sverdrup Basin, a β of ~0.55 is implied to thicken the crust from 24 to 44 km. Considering that the GU is ~150 km in width, this would suggest that over 100 km of shortening occurred during the Eurekan Orogen in this area.

Within the oceanic areas of both the Arctic Ocean and Baffin Bay, thin crustal values of 12–14 km are determined. This is thicker than would be expected for typical oceanic crust; however, since
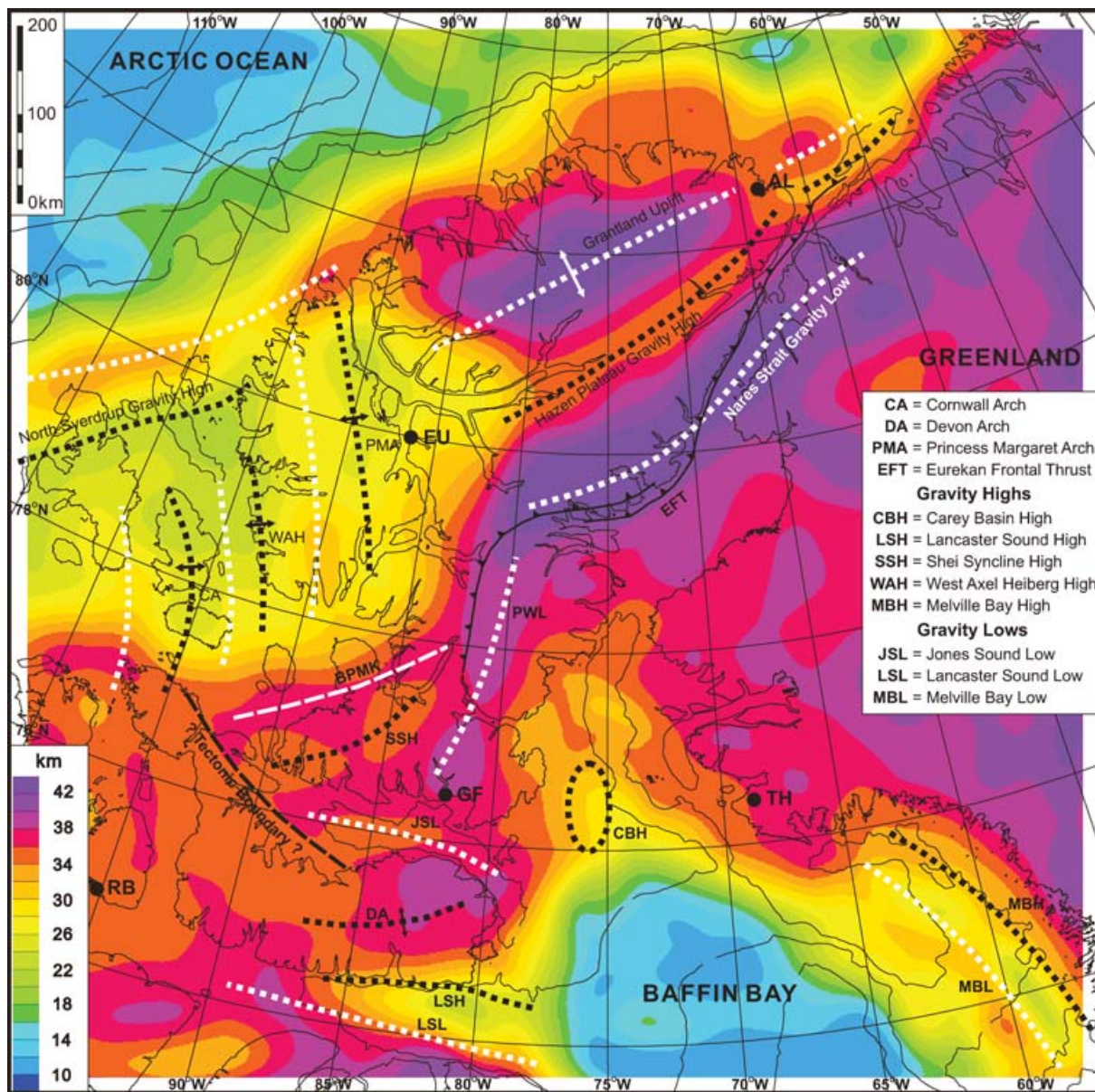
Figure 16. Crustal Thickness in the study area represents the difference between the Moho-depth and a depth-to-basement horizon determined by subtracting the sediment thickness values (Fig. 8) from the sub-ice surface (Fig. 7b). The axis of significant linear gravity highs (dotted black lines) and gravity lows (dotted white lines) are shown in the overlay. The thinned crustal region surrounding the Carey Basin High (CBH) is outlined by a grey dashed line. The inner estimate of the COB is shown with a red dashed line. Also shown is the position of the Eurekan Frontal Thrust (EFT) in northern Nares Strait, the Bjorne Peninsula Moho 'Keel' (BPMK; white dashed line), and an inferred tectonic boundary terminating the western end of the Shei Syncline and BPMK. Locations of receiver function stations as in Fig. 13.

the Moho-inversion modelling did not compensate for oceanic crust having a higher density than continental crust, this is not unexpected. The COB defined in Fig. 13 is also shown in Fig. 16, which is generally consistent with the 16 km crustal thickness contour (i.e β of >2); however, in Baffin Bay, adjacent to the Melville graben, the '16 km crustal thickness' contour is offset from the COB position defined by the 'crustal' Bouguer anomaly, suggesting that the COB is further seawards.

Crustal thinning is observed within most of the margin basins around Baffin Bay. The Melville Bay Ridge, separating the inner MBG and outer Kivioq Basin (KB), is between 32 and 34 km thick, only slightly thinner than 'average' (35 km) continental crust. Both the MBG and KB thin to ~22 km (with corresponding with a β of

~1.4). The crustal thickness within CB reaches a local minimum of ~26 km, slightly offset from the location of the CB Gravity High (shown as CBH in Fig. 16). It is surrounded by a broad area of crust ~32 km thick, suggesting that there has been broad area of systematic crustal thinning (with a corresponding β of ~1.2). Considering the well documented inversion features ('flower' structures) in this area (Jackson *et al.* 1992), it is very likely that the crustal rocks have also been influenced by the Eurekan plate convergence.

The Lancaster 'rift' basin has a minimum crustal thickness of 22 km (with a corresponding β of ~1.6). Although the basin is considered a 'failed rift arm' of the (Eocene) Baffin Bay spreading system, a β of only 1.6 indicates that, although severe rifting occurred, the basement rocks are unlikely to be oceanic crust.

Considerable crustal extension is, however, implied, perhaps accommodating as much as 40 km of separation between Devon Island and Baffin Island, enough to have significance for plate kinematic reconstructions (Oakey 2005). In contrast, there is no equivalent crustal thinning associated with the Jones Sound Basin (JSB), suggesting a different style (or age) of basin development.

4.3 Two-dimensional gravity modelling across the Nares Strait—Hazen Plateau gravity anomalies

A 2-D gravity model has been constructed along a profile (very close to Profile 3 in Fig. 12) that runs from KB onshore Ellesmere Island (Stephenson *et al.* 2003), crossing the Nares Strait–Hazen Plateau gravity anomalies. The model (Fig. 17a) comprises a sedimentary layer overlying a crystalline crust, divided into two uniform layers. The geometry of Palaeozoic strata from the balanced geological cross-section seen in Fig. 3 (Harrison & de Freitas 2007) has been used for constraint within the sedimentary layer. The densities of these Palaeozoic sediments were taken from samples and well logs and are tabulated in the legend of Fig. 3.

The modelling strategy was designed specifically to test whether the Nares Strait–Hazen Plateau gravity anomalies could be explained by sediment and upper crustal layer heterogeneities only, or Moho topography would also be necessary. In the model, the densities used for upper and lower crustal layers (2750 and 3000 kg m^{-3}) are based on regional gravity modelling by Sobczak *et al.* (1986), which are slightly higher than those used by Funck *et al.* (2006) further south, based on refraction velocities across southern Nares Strait (line FK; Fig. 13). The densities used minimize the contrast at the Moho and, hence, its gravity signature in the model. The Franklinian shelf sequence was divided laterally into three units, according to the mapped geology, allowing for an optimal effect of near-surface lateral density variations and minimizing those of the Moho. Numerous models were tested, with varying geometries and densities of the near-surface sedimentary units as well as the geometries of the Moho and the upper-lower crustal boundaries. In general, the boundary between the upper and lower crust was arbitrarily set parallel to the Moho surface, again to minimize the gravity contribution of Moho. The model shown in Fig. 17a (Profile 3) provides the best-fit to the observed gravity profile. Lateral variations in near-surface geology (e.g. shelf versus deep-water sedimentary provinces) make a significant contribution. However, even with the density (2760 kg m^{-3}) of the strata within the deep-water province of the Hazen Stable Block (Fig. 2) being an upper limit for these rocks, no reasonable models were found that satisfactorily matched the observed gravity field without a significant contribution from Moho topography.

To demonstrate the importance of the Moho in explaining the Nares Strait–Hazen Plateau gravity anomalies, the model seen in Fig. 17a is compared with a simple two-layer model with only a single density contrast at the Moho. The topography of the Moho is a profile extracted from Fig. 15, and the same densities used in the inverse modelling were adopted (ie. crust = 2670 kg m^{-3} and mantle = 3300 kg m^{-3}). Although the detailed fit of this model is clearly degraded compared with the model incorporating upper crustal and sediment layers, it is also apparent that Moho topography is capable in itself of explaining most of the long-wavelength component of the gravity field.

This inference is supported by additional modelling along the ten parallel profiles shown in Fig. 14 (located in Fig. 12). Simple two-layer models for profiles 5 and 7 are shown in Figs 17(b) and (c). In all models, the Moho geometry was extracted from the gravity inversion

Moho map (Fig. 15), with crust and mantle densities of 2670 and 3300 kg m^{-3} respectively. Again, variation in Moho depth along the profiles is almost sufficient to explain the observed Nares Strait–Hazen Plateau gravity anomalies, with the small 'high-frequency' residuals easily accommodated by shallower sources.

4.4 Isostasy and isostatic admittance ('*Q*') in the innuitian region

To assess the isostatic state of the Eurekan Orogen, the isostatic response function—or admittance (*Q*)—was calculated for the study area. *Q* is the ratio of the gravity power-spectrum and the gravity-topography cross-spectrum and provides an averaged, quantifiable expression to compare with theoretical models (e.g. Stephenson & Lambeck 1985; Verhoef & Jackson 1991). It has been determined from the Bouguer gravity field (Fig. 12) and the sub-ice topography (Fig. 7b), regridded to a 20 km cell size within the area indicated by the grey boxes in these figures, chosen to exclude deep-water areas with associated oceanic crust.

The averaged *Q* (points with error bars) for the study area is shown in Fig. 18. It exhibits near-zero values for wavenumbers greater than 0.06 km^{-1} (wavelengths less than 100 km), suggesting that the topography is not in local isostatic equilibrium. The best fitting theoretical admittance, based on a thin elastic plate (flexure) model with in-plane forces (e.g. Stephenson & Lambeck 1985), computed on the basis of minimization of (rms) errors, is also shown in Fig. 18 (grey line). Theoretical admittances were computing for reasonable ranges of various input parameters, including Moho depth (30–40 km), elastic plate flexural rigidity (10^{16}–10^{24} N m; the smaller values effectively representing local isostasy), and the absence or presence of an additional flexed density interface between an overlying sedimentary layer (0–10 km thickness) and crystalline crust. Additional tests for in-plane stresses (Stephenson & Lambeck 1985) were checked, but no statistically significant results were found. The best fitting model—which cannot be interpreted as a specific crustal model for any particular part of the study area but rather as a statistically best-fitting average model for the area as a whole—possesses a moderate flexural rigidity of 10^{22} N m, a crustal thickness of 30 km and no requirement for an additional shallower density interface.

The isostatic admittance *Q* is normally assumed to be directionally isostropic. However, Stephenson & Beaumont (1980) and Stephenson & Lambeck (1985) pointed out that, if the crust is subject to a non-topographic load with a specific orientation, including in-plane forces, or if the crust has some degree of mechanical/rheological anisotropy, then *Q* should be directionally anisotropic. This study area has features preserved from the Palaeozoic Franklinian margin as well as clearly developed regional Eurekan structures developed during unidirectional Eocene plate convergence. Accordingly, additional calculations were made to check for the possible presence of anisotropic admittance. The result, shown in Fig. 19a, shows the low wavenumber *Q* (wavelengths greater than 100 km) for the study area as a function of direction (calculated within a moving window every 10°). Long wavelength *Q* with azimuth 120°–150° (centred at 135°) indicates a clear tendency to be smaller than at other directions. No statistically significant anisotropy exists for wavenumbers higher than this.

The observed 135° anisotropy can be the result of either a reduction of gravity signal corresponding to this orientation and wavenumber or an increase in topographic signal. To visualize this, a comparison of the log$_{10}$ power-spectra for both are shown in Fig. 19b. Most of the power in the gravity spectrum corresponds
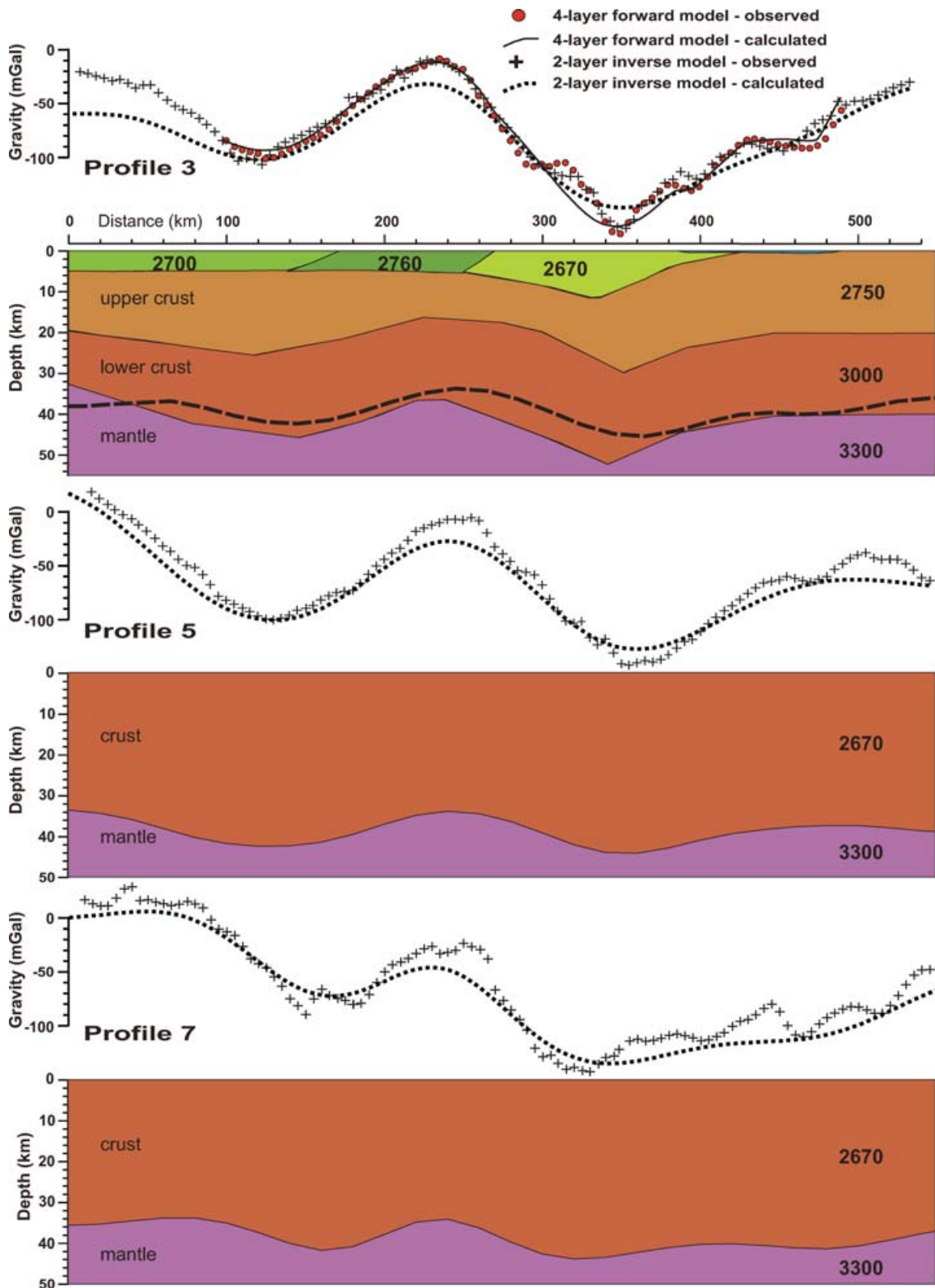
Figure 17. Density model (units of kg m^{-3}) with four layers (sediments, upper and lower crust and mantle) across the EFTZ by Stephenson *et al.* (2003) compared with the corresponding simple two-layer model based on the Moho inversion (upper panel). The observed gravity values for the two models differ slightly because the profiles are not exactly coincident. The thick dashed line overlying the model is the Moho calculated from the gravity inversion (cf. Fig. 15), in which densities of 2670 kg m^{-3} for crust and 3300 kg m^{-3} for mantle were adopted. Lower panels show two-layer (crust and mantle) models for profiles 5 and 7, derived from the Moho inversion (profiles located in Fig. 12). The observed gravity values are shown with '+' symbols and the calculated anomaly with a dotted black line as in the upper panel. Vertical exaggeration is approximately 4 : 1.
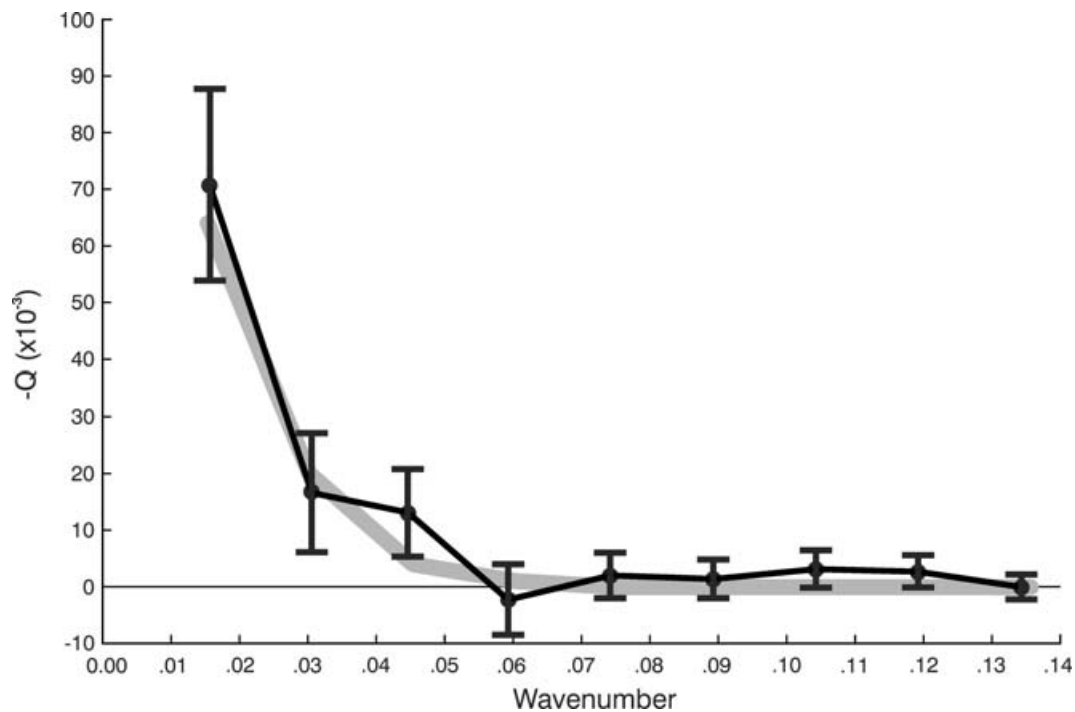
Figure 18. The isostatic response function (or admittance), Q, between Bouguer gravity and sub-ice surface for the study area (shown in Figs 7 and 12) with error bars. The best fitting theoretical model (grey line; see text for additional discussion) has a moderate crustal flexural rigidity of 10^{22} N m, a crustal thickness of 30 km and no mid- or upper-crustal density contrast.

to wavenumbers less than 0.06 km^{-1} (wavelengths > 100 km), with the drop-off in power being symmetric in all directions. In contrast, the power spectrum for the topography has pronounced lobes (shown by arrows) oriented at 135° for wavenumbers in the range 0.015–0.06 km^{-1} (i.e. wavelengths of 100–400 km). Thus, the observed power spectra suggest that the anisotropy is the result of a topographic signature that does not produce a corresponding gravity anomaly (at least to the degree that flexurally compensated topography would). Expressed physically, this means that there is less gravity signal at this wavelength in this direction, normalized in terms of the topography, than on average for the whole study area. That is to say, even though regional topographic grain might be aligned (perpendicular) to this direction, the isostatic admittance in such a case could still be isotropic if the respondent gravity field would also be so aligned. These results suggest a different form of isostatic compensation of topography in the 135° direction. Modelled in terms of the thin elastic plate model used earlier, a stronger flexural rigidity (10^{24} N m) is implied for the 135° direction, coincidently identical with the direction of Eurekan convergence during the Eocene. This is somewhat counte-rintuitive since the application of a horizontal force should weaken the lithosphere, rather than strengthening it. More realistically, the oriented topographic load produced from the Eurekan shortening is still undergoing post-orogenic 'collapse' and exerting anisotropic forces. With either explanation, this effective anisotropically 'stronger' lithosphere indicates that remnant interplate forces have not completely dissipated and a non-isostatic topographic load is still being supported.

5 SUMMARY OF RESULTS

The ability to differentiate between older Ellesmerian structures and unique or overprinted Eurekan deformation within the Canadian Archipelago has been an ongoing challenge. The presented gravity compilation over the Innuitian Region of the Canadian and Greenland Arctic provides new insights into the regional-scale crustal structure and the overprinting of Cretaceous–Palaeogene interplate tectonics culminating in the Eurekan Orogeny. Combined with newly compiled digital bathymetric, topographic and sediment thickness data, calculations of different gravity 'Bouguer' corrections have allowed improved correlations of onshore–offshore geological provinces, geometry of the sedimentary basins, and positions of continent–oceanic boundaries. Both 2-D and 3-D gravity modelling have allowed for quantitative assessment of regional variations in Moho-depth, crustal thickness and estimated β values for both areas of crustal thinning and thickening. Further, a Fourier domain transfer function (Q) analysis has provided estimates of lithospheric strength and degree of isostatic compensation. By comparison, the marginal basins around Baffin Bay are reasonable well modelled compared with the Sverdrup Basin and the Sverdrup Rim, where further investigations are required with improved mapping of the sediment thickness and better definition of the geometry of Cretaceous volcanic systems.

The main results of this study can be summarized as follows.

(1) A crustal thickness of ∼35 km represents 'normal' undeformed Archaean crust in the study area.

(2) The large amplitude linear gravity low—'Nares Strait Gravity Low (NSGL)'—extends obliquely across Nares Strait from northern Greenland to Ellesmere Island. This feature closely correlates with the distribution of the Palaeozoic Franklinian Margin sequences and is primarily the signature of a downwards flexure of the crust beneath a northwards thickening (Palaeozoic) sedimentary wedge.

(3) The NSGL is cross-cut by the Eurekan Frontal Thrust (EFT), which only locally enhances the gravity low in response to structural stacking of the Palaeozoic Franklinian Margin sequences during the Eurekan Orogeny.
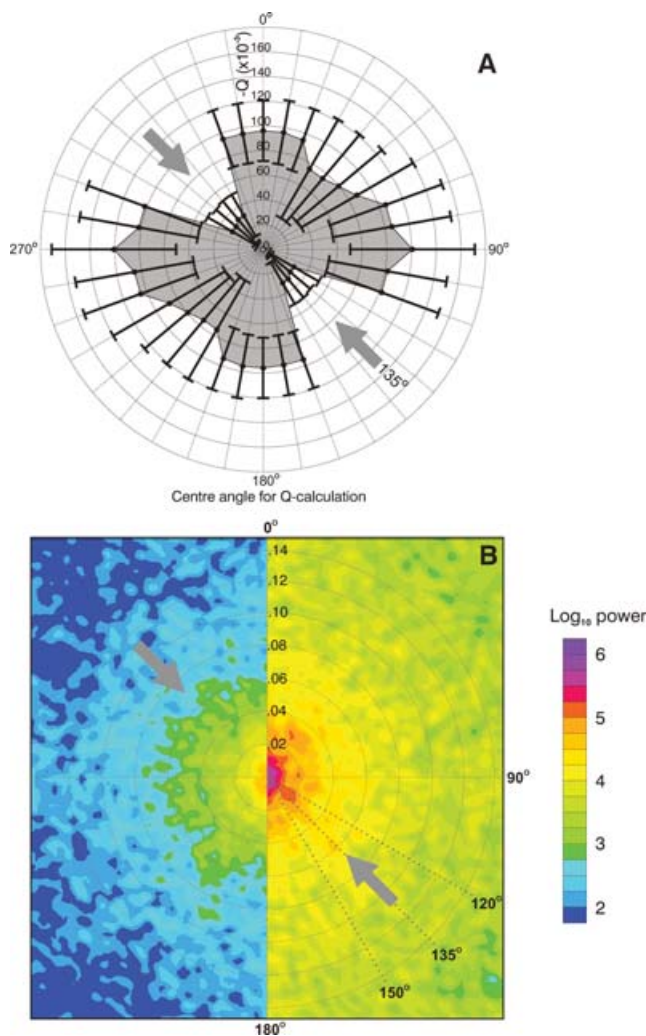
Figure 19. (a) Anisotropic *Q*-curves, calculated from 'pie-slices' with a central orientation incremented at 10° intervals. The smallest wavenumber (wavelength ∼400 km) from each curve is plotted with its corresponding error bar. An average value of ∼0.1 is observed for most orientations. Angles between 120° and 150° have a statistically significantly reduced value (∼0.03). Compared with theoretical curves, the results from the 135°-centred slice indicate a greater flexural rigidity (10^{24} N m) than in other directions. (b) The $\log_{10}$ power-spectra for the Bouguer gravity field (left-hand side) and the sub-ice surface (right-hand side) with wavenumbers. The increased power 'lobes' for the sub-ice surface oriented at 135° are shown with arrows.

(4) The NSGL can be mapped to the south along the lower amplitude Prince of Wales Gravity Low (PWL). The decreased crustal thickness values (∼38 km) along this feature suggest uplift and erosion of the Palaeozoic strata during the Eurekan Orogeny.

(5) Newly identified gravity signatures are correlated with geologically defined structural blocks north of the NSGL: the Hazen Plateau Gravity High (HPGH) corresponds with the low-lying topography of the Hazen Trough; and the Grantland Gravity Low (GGL) corresponds with the elevated topography of the Grantland Uplift (GU).

(6) The crustal thickness associated with the HPGH (∼35 km) corresponds with a 'stable' block of crust, apparently undeformed during Eurekan orogenesis.

(7) The crustal thickness associated with the GGL (>42 km) probably represents an area of significant crustal thickening during the Eurekan Orogeny associated with the exhumation of the easternmost part of the Sverdrup Basin. It cannot be excluded that some of the crustal thickening of the GU is ancestral, related to early Palaeozoic orogenesis.

(8) The Sverdrup Basin has an average crustal thickness of ∼24 km. The eastern and western areas of the basin are divided by a N–S oriented crustal block beneath Axel Heiberg Island ranging from ∼26 km thickness in the north to over 30 km in the south. This feature may represent crustal thickening in response to the Eurekan Orogeny.

(9) A newly defined N–S oriented linear gravity high is identified along the western edge of Axel Heiberg Island (WAH), approximately equidistant between the Cornwall (CA) and Princess Margaret (PMA) arches. The spacing between these structures is ∼100 km.

(10) The position of the continent–ocean boundary (COB) in both the Arctic Ocean and Baffin Bay has been refined and improved. The continental margin along the Melville Bay area of Greenland appears to be very wide.

(11) The Lancaster Basin overlies extremely thinned crust and is interpreted to be a failed 'rift arm' of the Eocene spreading system in central Baffin Bay. β values of ∼1.6 suggest significant extension across the basin (>40 km), enough to be relevant for plate kinematic reconstructions.

(12) There is no equivalent crustal thinning associated with the Jones Sound Basin, suggesting a different style (or age) of basin development.

(13) An intermediate flexural rigidity of 10^{22} N m was determined for the study area from its isostatic admittance (*Q*), with a notable anisotropy in *Q* corresponding with the direction of Eurekan convergence, suggesting that there remain forces from the plate convergence that are supporting an excess of topography without producing a corresponding gravity signature.

ACKNOWLEDGMENTS

REFERENCES

Asudeh, I., Forsyth, D.A., Stephenson, R.A., Embry, A.F. Jackson, H.R. & White, D., 1989. Crustal structure of the Canadian polar margin: results from the 1985 seismic refraction survey, *Can. J. Earth Sci.,* **26**(5), 853–866.

Balkwill, HR., McMillan, N. J., MacLean, B., Williams, G.L. & Srivastava, S.P., 1990. Geology of the Labrador shelf, Baffin Bay and Davis Strait, in *Geology of Canada, 2: Geology of the Continental Margin of Eastern Canada,* pp. 293–348, eds Keen, M.J. & Williams, G.L., Geological Survey of Canada (also in *Geology of North America,* Vol. I-1, Geological Society of America).

Bamber, J.L., Layberry, R.L. & Gogenini, S.P., 2001a. A new ice thickness and bed data set for the Greenland ice sheet 1: measurement, data reduction, and errors, *J. geophys. Res.,* **106**(D24), 33 773–33 780.

Bamber, J.L., Layberry, R.L. & Gogenini, S.P., 2001b. A new ice thickness and bed data set for the Greenland ice sheet 2: relationship between dynamic and basal topography, *J. geophys. Res.,* **106**(D24), 33 781–33 788.

Barton, P.J., 1986. The relationship between seismic velocity and density in the continental crust—a useful constraint?, *Geophys. J. R. astr. Soc.,* **87,** 195–208.

Chalmers, J.A. & Pulvertaft, T.C.R., 2001. Development of the continental margins of the Labrador Sea: a review, in *Non-Volcanic Rifting of Continental Margins: A Comparison of Evidence from Land and Sea,* Vol. 187, pp. 77–105, eds Wilson, R.C.L., Whitmarsh, R.B., Taylor, B. & Froitzheim, N., Special Publications – Geological Society of London.

Christie, R.L., 1976. Tertiary rocks at Lake Hazen, northern Ellesmere Island, *Geological Survey of Canada, Paper No. 76–1B,* pp. 259–262.

Dahl-Jensen, T. *et al.,* 2003. Depth to Moho in Greenland: receiver-function analysis suggests two Proterozoic blocks in Greenland, *Earth planet. Sci. Lett.,* **205,** 379–393.

Damaske, D. & Oakey, G.N., 2006. Volcanogenic sandstones as aeromagnetic markers on Judge Daly Promontory and Robeson Channel in the northern Nares Strait Region, *Polarforschung,* **74**(1–3), 9–19.

Darbyshire, F.A., 2003. Crustal structure across the Canadian High Arctic region from teleseismic receiver function analysis, *Geophys. J. Int.,* **152,** 372–391.

Davies, G.R. & Nassichuk, W.W., 1991. Carboniferous and Permian history of the Sverdrup Basin, Arctic Islands, in *Geology of Canada, 3: Geology of the Innuitian Orogen and Arctic Platform of Canada and Greenland,* pp. 345–367, ed. Trettin, H.P., Geological Survey of Canada (also *Geology of North America,* Vol. E, Geological Society of America).

Dawes, P.R. & Christie, R.L., 1991. Geomorphic regions, in *Geology of Canada, 3: Geology of the Innuitian Orogen and Arctic Platform of Canada and Greenland,* pp. 29–56, ed. Trettin, H.P., Geological Survey of Canada (also *Geology of North America,* Vol. E, Geological Society of America).

DePaor, D.G., Bradley, D.C., Eisenstadt, G. & Phillips, S.M., 1989. The Arctic Eurekan Orogen: a most unusual fold-and-thrust belt, *Geol. Soc. Am. Bull.,* **101,** 952–967.

Digital Chart of the World: Ice Boundaries, Edition 1, 1992. United States Defence Mapping Agency.

Ekholm, S., 1996. A full coverage, high-resolution, topographic model of Greenland computed from a variety of digital elevation data, *J. geophys. Res.,* **101**(B10), 21 961–21 972.

Embry A.F., 1991. Mesozoic history of the Arctic Islands, in *Geology of Canada, 3: Geology of the Innuitian Orogen and Arctic Platform of Canada and Greenland,* pp. 371–433, ed. Trettin, H.P., Geological Survey of Canada (also *Geology of North America,* Vol. E, Geological Society of America).

Forsyth, D.A., Mair, J.A. & Fraser, I., 1979. Crustal structure of the central Sverdrup Basin, *Can. J. Earth Sci.,* **16**(8), 1581–1598.

Forsyth, D.A., Broome, J., Embry, A.F. & Halpenny, J.F., 1990. Features of the Canadian Polar Margin, in *Arctic Geoscience,* Vol. 93, pp. 147–177, eds Webber, J.R., Forsyth, D.A., Embry, A.F. & Blasco, S.M., *Mar. Geol*.

Forsyth, D.A., Argyle, M., Okulitch, A. & Trettin, H.P., 1994. New seismic, magnetic, and gravity constraints on the crustal structure of the Lincoln Sea continent-ocean transition, *Can. J. Earth Sci.,* **31**(6), 905–918.

Forsyth, D.A., Asudeh, I., White, D., Jackson, R., Stevenson, R.A., Embry, A.F. & Argyle, M., 1998. Sedimentary basins and basement highs beneath the polar shelf north of Axel Heiberg and Meigen islands, *Bull.Can. Petrol. Geol.,* **46**(1), 12–29.

Funck, T., Jackson, H.R., Dehler, S.A. & Reid, I.D., 2006. A refraction seismic transect from Greenland to Ellesmere Island, Canada: the crustal structure in southern Nares Strait, *Polarforschung,* **74**(1–3), 97–112.

GTOPO30, 1999. Global 30 Arc Second Elevation Data, United States Geological Survey, National Mapping Division, EROS Data Center.

Geophysical Data Centre, 2000. Canadian National Gravity Database, Geological Survey of Canada, 615 Booth Street, Ottawa.

Harrison, J.C., 2006. In search of the Wegener Fault: re-evaluation of strike-slip displacements along and bordering Nares Strait, *Polarforschung,* **74**(1–3), 129–160.

Harrison, J.C. & de Freitas, T.A., 2007. *Geology, Agassiz Ice Cap, Ellesmere Island, Nunavut,* Geological Survey of Canada, Map 2104A, scale 1 : 125 000.

Harrison, J.C. *et al.*, 1999. Correlation of Cenozoic sequences of the Canadian Arctic region and Greenland; implications for the tectonic history of northern North America, *Bull. Can. Petrol. Geol.,* **47,** 223–254.

Harrison, J.C., Brent, T.A. & Oakey, G.N., 2006. A new geology map of the Nares Strait Region, *Geological Survey of Canada Open File Report No. 5278.*

Hearty, D. B., Seemann, D. A., Maye, P. & Jackson, R., 1996. Regional gravity survey of Ellesmere and Axel Heiberg islands, Northwest Territories. *Current Research: Part B, Geological Survey of Canada, Paper No. 1996–1B,* 73–79.

Hood, P., Bower, M.E., Hardwick, C.D. & Teskey, D.J., 1985. Direct geophysical evidence for displacement along Nares Strait (Canada-Greenland) from low-level aeromagnetic data: a progress report, *Current Research: Part A, Geological Survey of Canada, Paper No. 85–1A,* 517–522.

Jackson, H. R. & Koppen, L., 1985. The Nares Strait gravity anomaly and its implications for crustal structure, *Can. J. Earth Sci.,* **22**(9), 1322–1328.

Jackson H.R. & Oakey, G.N., 1990. Sedimentary thickness map of the Arctic Ocean, in *The Geology of North America, The Arctic Ocean,* Vol. L, map plate 5, eds Grantz, A., Johnson, L. & Sweeney, The Geological Society of America.

Jackson, H.R. & Reid, I., 1994. Crustal thickness variations between Greenland and Ellesmere Island margins determined from seismic refraction, *Can. J. Earth Scie.,* **31**(9), 1407–1418.

Jackson, H.R., Keen, C.E. & Barrett, D.L., 1977. Geophysical studies on the continental margin of Baffin Bay and in Lancaster Sound, *Can. J. Earth Sci.,* **14**(9), 1991–2001.

Jackson, H.R., Dickie, K. & Marillier, F., 1992. A seismic reflection study of northern Baffin Bay: implication for tectonic evolution, *Can. J. Earth Sci.,* **29**(11), 2353–2369.

Jackson, H.R., Hannon, T., Neben, S., Piepjohn, K. & Brent, T.A., 2006. Seismic reflection profiles from Kane to Hall Basin, Nares Strait. *Polarforschung,* **74**(1–3), 129–160.

Jones, M.T., Tabor, A.R. & Weatherall, P., 1994. GEBCO Digital Atlas: CD-ROM and Supporting Volume, *British Oceanographic Data Centre, Birkenhead, UK*.

Keen, C.E., Barret, D.L., Manchester, K.S. & Ross, D.I., 1972. Geophysical studies in Baffin Bay and some tectonic implications, *Can. J. of Earth Sci.,* **9**(3), 239–256.

Keen, C.E., Loncarevic, B.D., Reid, I., Woodside, J., Haworth, R.T. & Williams, H., 1990. Tectonic and geophysical overview, in *Geology of Canada, 2: Geology of the Continental Margin of Eastern Canada,* pp. 31–85, eds Keen, M.J. & Williams, G.L., Geological Survey of Canada (also *Geology of North America,* Vol. I-1, Geological Society of America).

Kerr, J. Wm., 1980. Structural framework of Lancaster Alacogen, Arctic Canada, *Geological Survey of Canada Bulletin,* **319,** 24 pp.

Koerner, R.M., 1977. Ice thickness measurements and their implications with respect to past and present ice volumes in the Canadian Hi Arctic ice caps, *Can. J. Earth Sci.,* **14**(12), 2697–2705.

Ludwig, J.W., Nafe, J.E. & Drake, C.L., 1970. Seismic refraction, in *The Sea,* Vol. 4, pp. 53–84, ed. Maxwell, A.E, Wiley Publishing, New York.

Marillier, F.M. & Verhoef, J.,1989. Crustal thickness under the Gulf of st. Lawrence, northern Appalachians from gravity and deep seismic data, *Can. J. Earth Sci.,* **26,** 1517–1532.

Maye, P., 1995. Operation BOUGUER-95: Ellesmere Island and Axel Heiberg Island gravity survey, *Mapping and Charting Establishment Field Operation Report No. 1995112.*

Mayr, U., de Freitas, T., Beauchamp, B. & Eisbacher, G., 1998. The geology of Devon Island north of 76°, Canadian Arctic Archipelago. *Geological Survey of Canada Bulletin,* **526,** 500 pp.

Miall, A.D., 1991. Late Cretaceous and Early Tertiary basin development and sedimentation, Arctic Islands, in *Geology of Canada, 3: Geology of the Innuitian Orogen and Arctic Platform of Canada and Greenland,*

pp. 437–458, ed. Trettin, H.P., Geological Survey of Canada (also *Geology of North America,* Vol E, Geological Society of America).

Nady, D., 1966. The gravitational attraction of a right rectangular prism, *Geophysics,* **31**(2), 362–371.

National Survey and Cadastre—Denmark (Kort & Matrikelstyrelsen), 1998. National Gravity Database, *Rentemerstervaj,* **8,** 2400 Copenhagen NV, Denmark.

Neben, S., Damm, V., Brent, T. & Tessensohn, F., 2006. New multi-channel seismic reflection data from Northwater Bay, Nares Strait: indications for pull-apart tectonics. *Polarforschung,* **74**(1–3), 77–96.

Niblett, E.R., DeLaurier, J.M., Law, L.K. & Plet, F.C., 1974. Geomagnetic variation anomalies in the Canadian Arctic I. Ellesmere Island and Lincoln Sea, *J. Geomag. Geoelectr.,* **26,** 203–221.

Oakey, G., 1994. A structural fabric defined by topographic lineaments: correlation with Tertiary deformation of Ellesmere and Axel Heiberg islands, Canadian Arctic, *J. geophys. Res.,* **99**(B10), 20 311–20 321.

Oakey, G. N., 2005. Cenozoic evolution and lithosphere dynamics of the Baffin Bay—Nares Strait region of Arctic Canada and Greenland, *PhD thesis.* 233pp. Vrije Universiteit, Amsterdam, the Netherlands, ISBN:0–09739355-0–2.

Oakey, G.N. & Chalmers, J.A., 2008. A new model for the Paleogene motion of Greenland relative to North America: a re-evaluation of the plate geometry of Baffin Bay, *J. geophys. Res,* submitted.

Oakey, G.N. & Damaske, D., 2006. Continuity of basement structures and dike swarms in the Kane Basin Region of central Nares Strait constrained by aeromagnetic data, *Polarforschung,* **74**(1–3), 51–62.

Oakey, G., Ekholm, S. & Jackson, H.R., 2001b. Physiography of the Innuitian Region Canadian and Greenland Arctic, *Geological Survey of Canada Open File No.* 3933D, scale 1:1,500,000.

Oakey, G., Hearty, B., Forsberg, R. & Jackson, H.R., 2001a. Gravity anomaly of the Innuitain Region, Canadian and Greenland Arctic, *Geological Survey of Canada Open File No.* 3934D, scale 1:1,500,000.

Okulitch, A.V. & Trettin , H.P., 1991. Late Cretaceous-Early Tertiary deformation, Arctic Islands, in *Geology of Canada, 3: Geology of the Innuitian Orogen and Arctic Platform of Canada and Greenland,* pp. 467–485, ed. Trettin, H.P. Geological Survey of Canada (also *Geology of North America,* Vol. E, Geological Society of America)

Okulitch, A.V., Dawes, P.R., Higgins, A.K., Soper, N.J. & Christie, R.L., 1990. Towards a Nares Strait solution: structural studies on southeastern Ellesmere Island and northwestern Greenland, *Mar. Geol.,* **93,** 369–384.

Parker, R.L., 1972. The rapid calculation of potential anomalies, *Geophys. J. R. astr. Soc.,* **31,** 447–455.

Peel J.S. & Christie, R.L., 1982. Cambrian-Ordovician Platform Stratigraphy: correlation around Kane Basin, in *Nares Strait and the Drift of Greenland: A Conflict in Plate Tectonics,* Vol. 8, pp. 117–135, eds Dawes, P.R. & Kerr, J.W, Meddelelser om Grønland, Geoscience.

Phillips, S.M., 1990. Deformation in a shear zone, Central Ellesmere Island, Canadian Arctic Archipelago: implications for regional tectonics, *Mar. Geol.,* **93,** 385–400.

Pilkington, M. & Crossley, D.J., 1986. Determination of crustal interface topography from potential fields, *Geophysics,* **51,** 1277–1284.

Reid, I. & Jackson, H. R., 1997. Crustal structure of northern Baffin Bay: seismic refraction results and tectonic implications, *J. geophys. Res.,* **102,** 523–542.

Rice, P.D. & Shade, B.D., 1982. Reflection seismic interpretation and seafloor spreading history of Baffin Bay. in *Arctic Geology and Geophysics,* Canadian Society of Petroleum Geologists Mem., 8, pp. 245–265, eds Embry, A.F. & Balkwill, H.R.

Ricketts, B. D., 1986. New Formations in the Eureka Sound Group, Canadian Arctic Islands, *Current Research: Part B, Geological Survey of Canada, Paper No. 86–01B,* 363–374.

Ricketts, B.D. & Stephenson, R.A., 1994. The demise of Sverdrup Basin: late Cretaceous- Paleogene sequence stratigraphy and forward modelling, *J. sediment. Res.,* **B64**(4), 516–530.

Roest, W.R. & Srivastava, S.P., 1989. Sea-floor spreading in the Labrador Sea: a new reconstruction, *Geology,* **17,** 1000–1003.

Saalmann, K., Tessensohn, F., Piepjohn, K., von Gosen, W., & Mayr, U., 2005. Structure of Palaeogene sediments in east Ellesmere Island; constraints on

Eurekan tectonic evolution and implications for the Nares Strait problem. *Tectonophysics,* **406**(1–2), 81–113.

Saalmann, K., Tessensohn, F., Von Gosen, W. & Piepjohn, K., 2008. Structural evolution of Tertiary rocks on Judge Daly Promontory, in *The Geology of Northeast Ellesmere Island Adjacent to Kane Basin and Kennedy Channel, Nunavut,* Geological Survey of Canada Bulletin, in press.

Sobczak, L.W., Mayr, U. & Sweeney, J.F., 1986. Crustal section across the polar continent-ocean transition in Canada. *Can. J. Earth Sci.,* **23**(5), 608–621.

Sobczak, L.W., Halpenny, J.F. & Henderson, D.M., 1991. Gravity interpretation along seismic refraction lines surveyed near the Canadian Ice Island during 1985. *Geological Survey of Canada Paper no. 90–12,* 23pp.

Srivastava, S.P., 1978. Evolution of the Labrador Sea and its bearing on the early evolution of the North Atlantic, *Geophys. J. R. astr. Soc.,* **52,** 313–357.

Srivastava, S.P. & Tapscott, C.R., 1986. Plate Kinematics of the North Atlantic, in *The Geology of North America, The Western North Atlantic Region,* 379–404 eds Vogt, P.R. & Tucholke, B.E.. *Geological Society of America,* Vol. M.

Stephenson, R. & Beaumont, C., 1980. Small-scale convection in the upper mantle and the isostatic response of the Canadian Shield, in *Mechanisms of Continental Drift and Plate Tectonics,* pp. 111–122, eds Davies, P.A. & Runcorn, S.K., Academic Press, London, UK.

Stephenson, R. & Lambeck, K., 1985. Isostatic Response of the Lithosphere with in-plane stress: application to central Australia, *J. geophys. Res.,* **90,** 5881–8588.

Stephenson, R.A. & Ricketts, B.D., 1990. Bouguer gravity anomalies and speculations on the regional crustal structure of the Eurekan Orogen, Arctic Canada, *Mar. Geol.,* **93,** 401–420.

Stephenson, R.A., Embry, A.F., Nakiboglu, S.M. & Hastaoglu, M.A., 1987. Rift-initiated Permian to Early Cretaceous subsidence of the Sverdrup Basin. in *Sedimentary Basins and Basin-Forming Mechanisms,* Vol. 5, pp. 213–231, eds Beaumont, C. & Tankard, A.J., Special Publication – Atlantic Geoscience Society.

Stephenson, R.A., Ricketts, B.D., Cloetingh, S.A. & Beekman, F., 1991. Lithospheric folds in the Eurekan orogen, Arctic Canada?, *Geology,* **18,** 603–606.

Stephenson, R., Harrison, C., Oakey, G. & Beekman, F., 2003, Gravity modelling in the Innuitian Orogen on north-eastern Ellesmere Island, in *Proceedings of Fourth International Conference on Arctic Margins (ICAM-IV) meeting,* Tromso, Norway. Program Abstracts Volume, 70–78.

Trettin, H.P., 1989. The Arctic Islands (Ch.13), in *The Geology of North America, An overview,* Vol. A, pp. 349–370, eds Bally, A.W. & Palmer, A.R., Geological Society of America.

Trettin, H.P., 1991. Silurian—early Carboniferous deformational phases and associated metamorphism and plutonism, Arctic Islands, in *Geology of Canada, 3: Geology of the Innuitian Orogen and Arctic Platform of Canada and Greenland,* pp. 295–341, ed. Trettin, H.P., Geological Survey of Canada (also *Geology of North America,* Vol. E, Geological Society of America)

Verhoef, J. & Jackson, H.R., 1991. Admittance signatures of rifted margins: examples from eastern Canada, *Geophys. J. Int.,* **105,** 229–239.

Wegener, A., 1915. Die Entstehung der Kontinente un Ozean. *Friedr. Vieweg & Sohn, Braunschweig,* 94p.

Whittaker, R.C. & Hamann, N.E., 1995. The Melville Bay area, North-West Greenland—the first phase of petroleum exploration, *Rapp. Grønland geol. Unders.,* **165,** 28–31.

APPENDIX A: CANADA'S NATIONAL ENERGY BOARD (NEB) DATA SOURCES FOR SEDIMENT THICKNESS MAPS

Lancaster Sound (6 maps):
Norlands Petroleum Limited, 1974;
Time structure map: Horizon C, Base Low Velocity Strata;

Two-Way Reflection Time Below Sea Level Reference;
1:50,000 scale maps, Universal Transverse Mercator Projection;
Contour Interval: 0.05 s;
NEB assessment file no. 511–09-09–09.

Lancaster Sound (3 maps):
Norlands Petroleum Limited, 1976;
Time structure map: Horizon C, Base Low Velocity Strata;
Two-Way Reflection Time below Sea Level Reference;
1:50,000 scale maps, Universal Transverse Mercator Projection;
Contour Interval: 0.05 s;
NEB assessment file no. 511–09-12—018.

Lancaster Sound (2 maps):
Baffin Bay Petroleum Limited, 1974;
Time structure map: Horizon G, Near Seismic Basement;
Two-Way Reflection Time below Sea Level Reference;
1:250,000 scale maps, Universal Transverse Mercator Projection;
Contour Interval: 0.10 s;

NEB assessment file NEB no. 562–09-09–002.
(NEB assessment file report includes tabulated sonobouy velocity data.)

North Baffin Bay and South Baffin Bay (2 maps):
Gulf Oil Canada Limited, 1974;
Time structure map: Horizon C, Base Low Velocity Strata;
Two-Way Reflection Time below Sea Level Reference;
1:200,000 scale maps, Universal Transverse Mercator Projection;
Contour Interval: 0.25 s;
NEB assessment file NEB no. 002–09-12–099.

Kane Basin (1 map):
Great Plains Development Company of Canada Limited, 1976;
Time structure map: Horizon A, Near Base-Palaeogene;
Two-Way Reflection Time below Sea Level Reference;
1:250,000 scale maps, Universal Transverse Mercator Projection;
Contour Interval: 0.10 s;
NEB assessment file NEB no. 76–9-10–74-4.